# NEUTRAL PRODUCTS FROM GAS PHASE REARRANGEMENTS OF SIMPLE CARBOCATIONS

Thomas Hellman Morton

**OUTLINE**



**Advances in Gas-Phase Ion Chemistry**
**Volume 4, pages 213–256.**

## ABSTRACT

Analyzing the neutral products from ionic reactions in the gas phase provides information that cannot be gained by mass spectrometric methods alone. Neutrals have been recovered using three general techniques for generating ions in sufficient quantities: nuclear decay of multiply tritiated precursors, $\gamma$-radiolysis studies, and electron bombardment flow (EBFlow) experiments. Analyses of the uncharged reaction products of ion–molecule reactions are most effectively interpreted in conjunction with parallel mass spectrometric investigations. Taken together, these combined studies demonstrate the propensity of gaseous cations to undergo similar sorts of isomerizations as have been reported in condensed media. The absence of solvent and counterions makes it possible to produce ions in the gas phase that cannot be formed in solution. Despite the difference in reaction medium, the same two general categories of rearrangement—ring closure/ring opening and atom/group transfer—account for the variety of ion structures that give rise to the observed neutral products.


## I. INTRODUCTION

Cationic rearrangements play a major role in organic and biological chemistry. For example, they account for the enormous variety of carbon skeletons found in natural products. Those rearrangements do not typically take place in bulk solution. Instead they occur within enzyme active sites. The number of enzymes is at least as great as the number of structures they produce, yet it has long been recognized that nearly all cationic rearrangement pathways fall into two categories: ring closure/ring opening and atom/group transfer.[1–3] Both move the electric charge onto a new center.

How can such a limited repertoire of mechanisms lead to the vast range of naturally occurring molecular structures? Biologists are endeavoring to answer that question by genetic manipulation,[4] but the outlines of the answer are already apparent: controlling the microscopic environment of the cation by steric hindrance, positioning of counterions, orientation of permanent dipoles and proximity of induced dipoles determine which of many possible avenues a cation follows. Guiding the rate of capture of the ion and the site at which it occurs must also play an important role in stopping the reaction at just the right point. Implicit in this picture is the notion that most carbocations enjoy many thermally accessible reaction pathways, which are governed by conformation and electric fields on the molecular scale. Understanding what cations do in the absence of solvent and counterions provides a guide to the consequences of these external effects.

From a historical perspective, their relevance to natural products explains why cationic rearrangements have attracted chemists' attention for more than a century. Recent years have seen a focus on increasingly simple structures, with the development of strategies to examine isolated cations. Out of such experiments, a clearer picture is emerging of their intrinsic reactivity, which offers insight as to how environment affects mechanism. NMR studies in non-nucleophilic solvents, and mass spectrometric studies in the gas phase, have greatly expanded our knowledge, but there are many categories of simple ions whose chemistry cannot be explored by these techniques. Some species are inaccessible for NMR studies because their precursors form different positively charged species under highly acidic conditions, or else the cations rearrange to more stable structures too rapidly. Mass spectrometry by itself typically gives limited information regarding ion structures. A variety of approaches have interrogated the neutral products that result from cationic rearrangements, with a view towards examining isomer and (in the case of labeled ions) isotopomeric distributions. The two categories of rearrangement have been explored in this fashion. Sections III–IV of this chapter will focus on carbocations with an even number of electrons. Where appropriate, previously unpublished computational results using density functional calculations (B3LYP/6-31G** with zero point energy correction[5]) from the author's laboratory supplement discussions of experimental results. First, however, it will be useful to clarify some general aspects of branching between competing pathways.

## II. THERMODYNAMIC VERSUS KINETIC CONTROL

The first question to be posed in discussing rearrangement chemistry concerns whether a given step exhibits thermodynamic or kinetic control, i.e. whether the distribution of products reflects equilibrium proportions. This issue arises at several stages in a reaction sequence: the production of ions, their isomerizations, and the processes by which ions become neutralized. Ions often form (e.g. by bond cleavage) under conditions that reflect thermodynamic control, while their ultimate neutralization (e.g. gas phase proton transfer) tends to operate with kinetic control.

### A. Bond Cleavage: Homolysis, Heterolysis, and Mesolysis

Direct ionization of neutral precursors typically produces ions with an odd number of electrons. Even-electron ions form subsequently, either by

bond cleavage or via ion–molecule reactions. With regard to single bond cleavages, the terms homolysis and heterolysis are well understood. When the electron pair in a covalent bond splits between two fragments, the cleavage is a homolysis. When one fragment retains both electrons, the cleavage is a heterolysis. Application of this terminology to ions is, in many cases, straightforward. If the electric charge in the starting material can be viewed as localized on one side of the breaking bond, the position of the charge after cleavage determines whether homolysis or heterolysis has taken place. When the charge stays on the same side, the bond fission is a homolysis. When the charge migrates to the other side, the bond fission is a heterolysis.

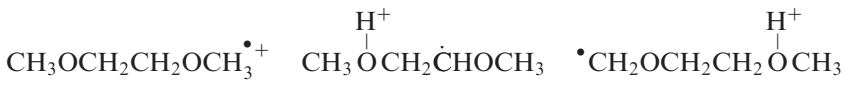

**A** **B** **C**

A simple example illustrates this distinction for the set of radical cations **A–C**. When prepared at low ionizing energies, the molecular ion of 1,2-dimethoxyethane (**A**) decomposes as though it rearranges to a mixture of the two distonic ions **B** and **C** drawn above.[6] In both distonic ions, the positive charge is localized on the protonated methoxy group. Ion **B** loses neutral methanol to yield ionized $CH_2{=}CHOCH_3$. In other words, the charge moves from methanol to the other side of the breaking bond, and the cleavage is a heterolysis.

Ion **C** loses neutral formaldehyde to form the distonic radical ion $^{\bullet}CH_2CH_2O(H)CH_3^+$. In this case, the positive charge is retained by the fragment that originally carried it, and the cleavage is a homolysis. The cleavage of the carbon–carbon bond of **A** (which represents the base peak in the 70 eV mass spectrum) into $CH_3O{=}CH_2^+$ and $CH_3OCH_2{\cdot}$ cannot be be classified as homolysis or heterolysis, because the charge is completely delocalized between the two oxygens in the molecular ion. This is an example of what Maslak has termed a mesolysis,[7] which he defines as the cleavage of a radical ion into a radical and an ion. While examples of homolysis and heterolysis have been included under this rubric,[7,8] as well, it would seem to make more sense (at least in the context of gas phase ion chemistry) to restrict mesolysis to describe only those cleavages that cannot be categorized as either homolysis or heterolysis.

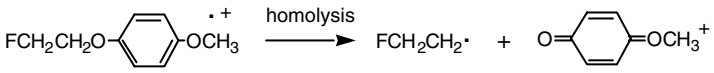


(1)

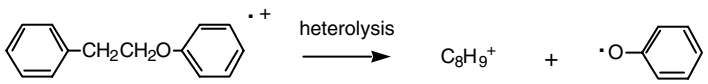


(2)

Now consider instances of homolysis and heterolysis that produce even-electron ions from odd-electron precursors. The cleavages of the two ionized molecular ions in equations 1 and 2 correspond to the most abundant bond fissions in the mass spectra of the corresponding aryl ethers. Each one yields a neutral radical and a cation. Since the charge can be viewed as being localized in the aryloxy group in both starting materials, the fission in equation 1 represents a homolysis, while the one in equation 2 is a heterolysis. Bond cleavages of radical cations (be they homolytic, heterolytic, or mesolytic) tend to exhibit thermodynamic control, in the sense that the charge resides on the most easily ionized fragment. This is sometimes called the Audier–Stevenson rule.[9,10]

## B. Reaction Path Degeneracy

When a reaction does not produce an equilibrium distribution of products, it is exhibiting some form of kinetic control. In one limiting case, kinetic control gives relative yields that are completely insensitive to thermodynamic considerations. Under such circumstances, the product ratio reflects the degeneracies of the competing reaction paths. In 1978, Coulson[11] and Pollak and Pechoukas[12] published back-to-back papers, in which they prove a simple algorithm for determining the reaction path degeneracy of a single-step reaction. The algorithm can be formulated as follows:

(*i*) Find the symmetry numbers $\sigma$ of the reactant and of the transition state;
(*ii*) Multiply $\sigma$ by 1/2 if the corresponding species is not superimposable on its mirror image (i.e. is chiral, or, to use the terminology of Pollak and Pechoukas[12], is "optically active") to get a weighted symmetry number;
(*iii*) Divide the weighted symmetry number of the reactant by that of the transition state to get the reaction path degeneracy for the forward direction.

The first step applies rigorously to overall molecular rotations. At temperatures where internal barriers can be neglected (typically $<10$ kT; e.g. for most single-bond torsions at room temperature), the algorithm can be extended to include internal rotations. A simple example illustrates the use of the algorithm: the unimolecular dissociation of ionized isopropyl

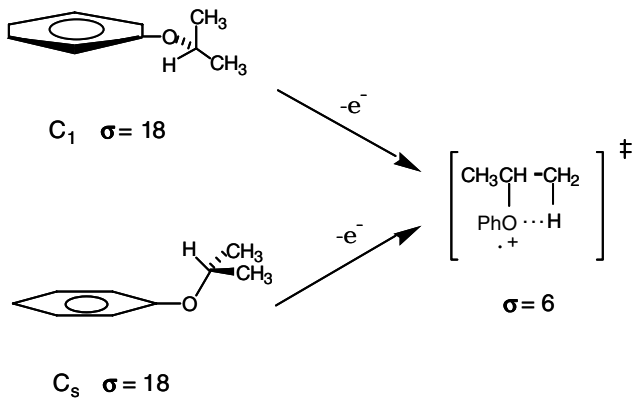


***Scheme 1.***

phenyl ether into ionized phenol and neutral propene. Ab initio calculations indicate that the neutral ether has two stable conformations, one with a plane of symmetry ($C_s$) and one without ($C_1$), as Scheme 1 illustrates. Laser REMPI spectroscopy of a supersonically cooled jet confirms the ab initio prediction that the $C_1$ is lower in energy.[13]

A transition state for concerted 4-center elimination from the molecule is depicted to the right in Scheme 1,[14] and we consider here the reaction path degeneracy for each conformation as it passes through this transition state. Internal rotation about the phenyl–oxygen bond is considered explicitly as a 2-fold free rotor in both conformations of the reactant as well as in the transition state. The $C_1$ and $C_s$ reactants each possess, in addition, a pair of methyl rotors, for net symmetry numbers $\sigma = 18$. The transition state retains only one of these methyl rotors, for a net symmetry number $\sigma = 6$. The transition state and the $C_1$ reactant are both chiral, and the corresponding reaction path degeneracy is 3. The $C_s$ reactant is achiral, so the reaction path degeneracy for this conformation is 6.

In other words, elimination from the more symmetrical structure is favored by naive statistics (even though this conformation happens to be energetically less accessible). The number of energetically equivalent pathways (as would be obtained by enumeration of equivalent hydrogens) is the same as the reaction path degeneracy: the methyl groups in the $C_s$ conformation are rendered equivalent by the plane of symmetry, while in the $C_1$ conformation the methyl groups are distinguishable. While the reaction path degeneracy is not always necessarily the same as the number of chemically equivalent atoms,[12] it turns out that few of the examples where the two methods disagree are chemically realistic.

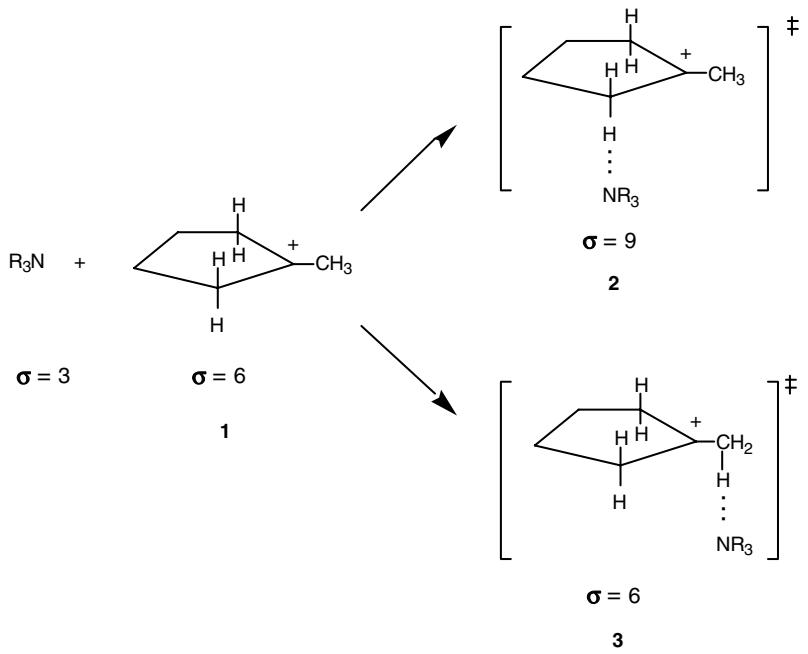


***Scheme 2.***

We now turn to the competition between two transition states with different symmetry numbers. Consider the reaction of the 1-methylcyclopentyl cation, **1**, with a symmetrically substituted amine $R_3N$, drawn in Scheme 2. Cation **1** is produced in both solution and the gas phase via unimolecular rearrangement of the cyclohexyl cation.[15] At room temperature, the gaseous cyclohexyl cation has a lifetime on the order of 1 ms before undergoing this exothermic isomerization.[16,17]

Two alternative types of intermediate (which we call the Eigen model and the Lewis model[18,19]), could describe the mechanism for the Brønsted acid–base reaction. The Eigen model supposes strong hydrogen-bonding between the acidic cation and the neutral base prior to proton transfer. The Lewis model supposes a covalent Lewis acid–base complex. In contrasting the predictions of these two models, we neglect internal rotation about N–R or within the R-groups, since that contribution does not change in going from reactant to transition state. Carbocation **1** has a planar skeleton and $C_s$ symmetry, with $\sigma = 6$ since it possesses both an internal 2-fold rotor (the 5-member ring) and a methyl rotor, connected by an $sp^2$–$sp^3$ carbon–carbon single bond. The $R_3N$ molecule has an overall $C_3$-axis of symmetry and $\sigma = 3$. Thus the net symmetry number of the reactants is 18.

The Eigen model requires two different hydrogen-bonded intermediates corresponding to the two alkene products that are formed. Each intermediate leads to a different transition state, structures **2** and **3** drawn in Scheme 2. The former, **2**, leads ultimately to 1-methylcyclopentene as the final product. This transition state has no overall molecular symmetry, but retains the methyl rotor as well as free rotation about the carbon–nitrogen single bond for a net symmetry number $\sigma = 9$. Because transition state **2** is chiral, the reaction path degeneracy is equal to $(18/\frac{9}{2}) = 4$.

The latter transition state, **3**, leads to methylenecyclopentane as the final product. This transition state retains $C_s$-symmetry, the 2-fold internal rotor, and 3-fold internal rotation about the carbon–nitrogen bond, for a net symmetry number $\sigma = 6$. Since neither the reactant nor this transition state is chiral, the reaction path degeneracy is $(18/6) = 3$.

Let us compare the ratio of reaction path degeneracies in Scheme 2 (4/3) to the ratio expected for net proton transfer via the Lewis model, which proceeds via unimolecular decomposition of a single intermediate, the quarternary ammonium ion **4** in Scheme 3. The reactive intermediate has $C_s$-symmetry and two internal 3-fold rotors, for $\sigma = 9$. Ion **4** can dissociate via two competing transition states, **5** and **6**, both of which

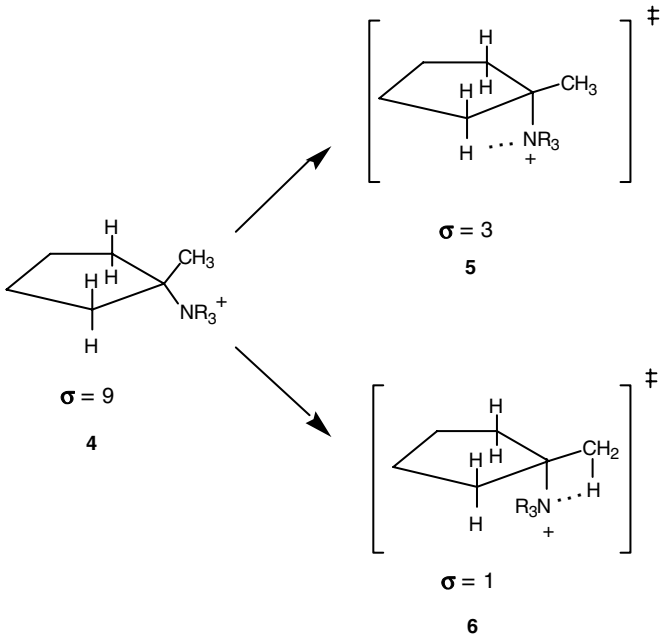


***Scheme 3.***

freeze internal rotation about the carbon–nitrogen single bond. Transition state **5** (which leads to 1-methylcyclopentene) retains its methyl rotor ($\sigma = 3$) but is chiral. Hence the reaction path degeneracy is 6. In terms of statistical factors this corresponds to the two chemically equivalent hydrogens *cis* to the nitrogen, multiplied by three equivalent orientations of the $NR_3$.

Transition state **6** (which leads to methylenecyclopentane) retains the plane of symmetry, but has no internal rotors. Therefore the reaction path degeneracy is 9. Thus, the predicted ratio of reaction path degeneracies is $6/9 = 2/3$, a factor of two different from that determined for Scheme 2. Repeated measurements of the 1-methylcyclopentene/methylenecyclopentane product ratio from the gas phase reaction of **1** with tertiary amines[15,19] (where energy barriers are negligible) give branching ratios within experimental error of 4/3 (e.g. $1.34 \pm 0.02$ for R = methyl[19]), which has been taken to argue in favor of the Eigen model rather than the Lewis model. With weaker bases, the product distribution shifts in the direction of the thermodynamically favored product.[18,19]

### C. Distinguishing Transposition from Randomization

In principle, isotopic labeling ought to permit the neutral products of a cationic reaction to be deduced from mass spectrometric measurements alone. As an example, the elimination reaction drawn in Scheme 1 yields a mixture of *cis* and *trans* alkenes when the alkyl group has $>3$ carbons. If the reaction passes through transition state drawn in Scheme 1 (called a *syn*-transition state), the ratio of alkene isomers from the stereospecifically deuterated precursors in Scheme 4 should correspond to the ratio of $PhOH^{\bullet +}$ to $PhOD^{\bullet +}$ observed in the mass spectrum.[20]

Two caveats apply to such an inference. First, the deuterium label affects the outcome of the reaction, and its kinetic isotope effect must be taken into account. Second, many cations tend to scramble their atoms (although the radical ions in Scheme 4 do not do so). One must therefore survey additional isotopically labeled analogues in order to ensure that scrambling is not taking place.[21]

Deuterium scrambling can arise from different types of exchange, as Scheme 5 portrays for an idealized molecule containing a dideuterated and an undeuterated methylene group. Positional interchange transposes the labeled and unlabeled carbon atoms (in general, by passing through a structure where, in the absence of label, they would be chemically equivalent). This implies that carbon–deuterium bonds do not break, and the net result is illustrated at the top of Scheme 5. If a carbon happened to be isotopically labeled as well, the hydrogens originally attached to it would

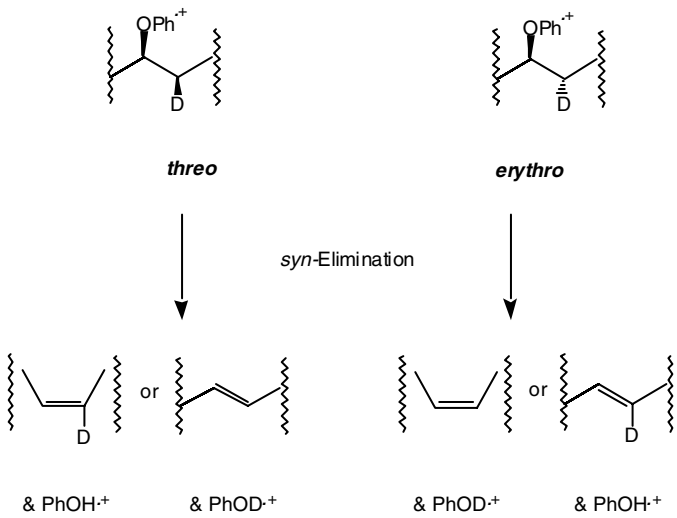


*Scheme 4.*

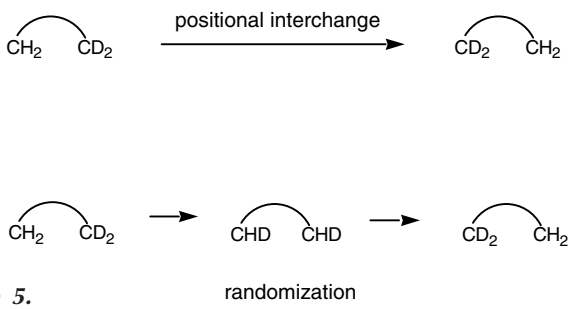


*Scheme 5.*

be observed not to have shifted. Randomization, by contrast, designates a process in which hydrogens move back and forth, leading to the outcome shown at the bottom of Scheme 5. The two types of exchange can be differentiated by the fact that species with CHD groups form during randomization, but not during positional interchange.

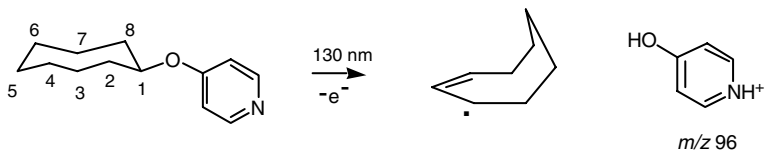


(3)

Mass spectrometry by itself cannot usually tell what positional isomers are present in a mixture. In favorable cases, however, it is possible to differentiate between positional interchange and randomization by analyzing product ion distributions. The double hydrogen transfer in equation 3 represents a case in point. Photoionization of cyclooctyl 4-pyridyl ether at 9.5 eV gives a high yield (approximately half of the total ionization) of protonated 4-hydroxypyridine ($m/z$ 96), along with a neutral product that is presumed to be cyclooctenyl radical (for which the most favorable conformation is drawn). The calculated (B3LYP/6-31G**) appearance energy for this dissociation is 7.5 eV, far below that calculated for production of free cyclooctyl cation (AE = 9.3 eV). On one hand, deuteration of the cyclooctyl ring at positions 1 or 5 leads to a very low level of deuterium incorporation into the ion. On the other hand, perdeuteration at positions 2 and 8 or at positions 4 and 6 leads to a substantial increase in the deuterium content of the ion, and the $d_0$ ($m/z$ 96) : $d_1$ ($m/z$ 97) : $d_2$ ($m/z$ 98) ion intensity ratios are nearly the same for both tetradeuterated starting materials.[22] Does this represent positional interchange or randomization?

Scheme 6 depicts a way to test whether randomization takes place, assuming that the double hydrogen transfer occurs in two steps. Suppose that randomization of $m$ hydrogens with $n$ deuteria takes place in the parent molecular ion, $M^{\bullet +}$, prior to hydrogen transfer. The first step can transfer either an H (to give intermediate **I**) or a D (to give intermediate **II**). If the ratio of **I** to **II** does not vary with time and if the second step obeys first-order kinetics, then the kinetic isotope effect $k_H/k_D$ can be extracted from the experimental ion intensity ratios $[d_0/d_2]$ and $[d_1/d_2]$ by means of the expression in equation 4:

$$k_H/k_D = \frac{n-1}{2n}\left\{[d_1/d_2] + \left([d_1/d_2]^2 - \frac{4mn[d_0/d_2]}{(n-1)/(m-1)}\right)^{1/2}\right\} \qquad (4)$$

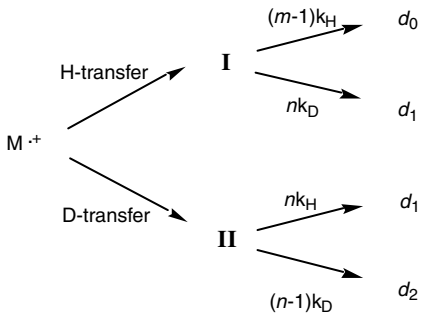


***Scheme 6.***

It turns out that all positive definite choices for $m$ and $n$ give imaginary values for $k_H/k_D$ when the experimental values of the ion intensity ratios are substituted into the equation.[22] In other words, simple randomization cannot account for the fact that the two tetradeuterated isomers give the same observed proportions of $d_0$, $d_1$, and $d_2$ fragment ions.

As is well known, kinetic arguments can be used to disprove mechanistic hypotheses (as in this instance), but never to prove them. The validity of first-order kinetics has been experimentally verified for monoenergetic ions,[23] but the general applicability to ions with a distribution of internal energies has been questioned.[24] Conditions under which first-order kinetics represent a usable approximation have been discussed,[25] and kinetic isotope effects (having positive definite values) have been extracted from experimental data for a number of unimolecular decompositions of ions produced by photoionization.[14,26–28] Our interpretation of the dissociation in Scheme 6 in terms of positional interchange is treated in the next section.

### D. Formation of Ion–Neutral Complexes versus Simple Bond Fission

An ion–neutral complex is defined as an aggregate of an ion with one or more neutrals, in which at least one of the partners has a rotational degree of freedom about an axis perpendicular to the intermolecular direction. This definition is known as the ''reorientation criterion'',[30] and the characteristic degree of freedom within a complex has sometimes been called ''planetary motion''.[31] Ion–neutral complexes can form either as a result of a bimolecular reaction or from unimolecular dissociation. Theory suggests that some closed shell clusters, where one of the partners has tetrahedral symmetry (such as $P_4 \cdot Li^{+}$[31] or the proton-bound dimer of ammonia and fluoromethane,[32] which have been observed in the mass spectrometer), constitute stable ion–neutral complexes. Since fluorine does not tend to form strong hydrogen bonds, the ammonium ion within species such as $NH_4^+ \ldots FH$[33] or $NH_4^+ \ldots FCH_3$[32] at room temperature ought to enjoy virtually free rotation in three dimensions. Directed valence (such as operates in conventional hydrogen bonds) is therefore largely absent, and the bonding must be viewed as mostly ionic in character.

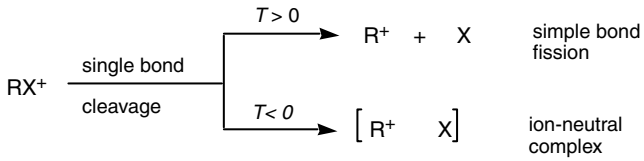


(5)

Short-lived ion–neutral complexes are created unimolecularly when bonds sever in parent ions and the fragments do not have enough kinetic energy to completely escape the electrostatic attraction between them. This can be thought of as a negative translational kinetic energy release ($T < 0$), as equation 5 represents schematically for cleavage of an R–X single bond. In a number of cases, simple bond fission (positive translational kinetic energy release, $T > 0$) and formation of ion–neutral complexes compete with one another. Transient ion–neutral complexes reveal their existence when they undergo an ion–molecule reaction between the partners faster than they collapse back to a covalently bound structure. Isotopic scrambling within the ionic partner frequently displays aspects characteristic of a free ion, but the lifetime of the complex is usually too short to permit skeletal rearrangement.[34] In the case of equation 3, photoionization was performed at a long enough wavelength that simple bond fission cannot compete with effectively. Instead, cyclooctyl cations are formed in ion–neutral complexes with 4-pyridyloxy radicals.

Were it possible to look at the cyclooctenyl radicals from equation 3, the neutrals produced by the tetradeuterated precursors would be expected to contain $sp^3$ carbons with $CH_2$ or $CD_2$, but no CHD groups. It has not yet proven possible to examine those radicals directly, but this deduction arises from the arguments outlined in the previous section. The positional interchange agrees with what would be predicted for the [cyclooctyl cation $^{\bullet}OC_5H_4N$] ion–neutral complex to the left in Scheme 7, whose subsequent Brønsted acid–base reactions give the ion–neutral complexes containing the forms of cyclooctene that are drawn in brackets. The cyclooctyl cation is known (from solution phase NMR studies[35]) to have a bridged structure,

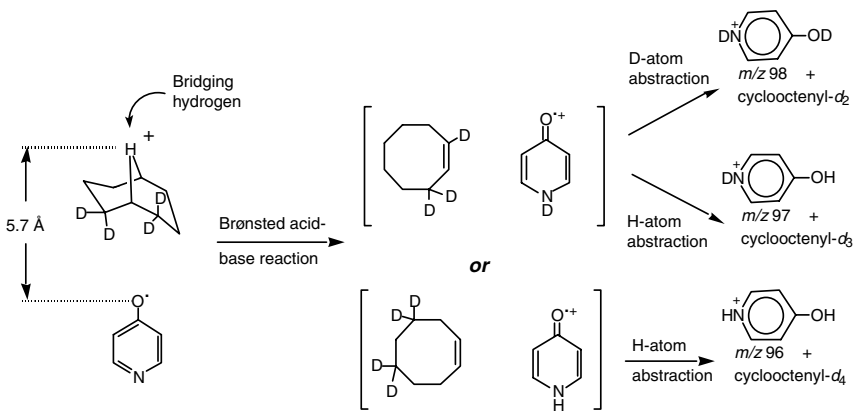


***Scheme 7.***

which confers a plane of symmetry upon the carbon skeleton that does not exist in monosubstituted cyclooctanes.

The observed proportions of $d_0$ ($m/z$ 96), $d_1$ ($m/z$ 97), and $d_2$ ($m/z$ 98) ions result from a normal kinetic isotope effect on the order of 3.5 for the Brønsted acid–base reaction followed by a $k_H/k_D$ of 2.8 for the subsequent atom abstraction. Cyclooctyl cations acquire symmetry due to the bridging hydrogen, as depicted, which accounts for the fact that both of the tetradeuterated precursors give the same product ion intensity ratios. After the Brønsted acid–base step, however, the cyclooctene-containing complexes are discrete and non-interconverting, which accounts for why the randomization model (equation 3) fails for this reaction.

Since an ion–neutral complex does not exhibit directed valence between the partners, it cannot be said to have an equilibrium structure. Some discussion of the interaction seems warranted at this point. The simplest physical picture for an ion–neutral complex portrays it in terms of a point charge and a point dipole. Density functional (DFT) calculations have tested this approximation for the [cyclooctyl cation $^{\bullet}OC_5H_4N$] complex. The permanent dipole moment of a 4-pyridyloxy radical in its lowest electronic state is calculated to be 1.1 Debye, and the calculated exact polarizability in the C–O bond direction is $\alpha_{zz} = 11.4$ Å$^3$ (at the B3LYP/6-31G** level). The geometry shown in Scheme 7 (which is constrained to have a plane of symmetry and corresponds to a center-of-charge to center-of-charge distance of 6.8 Å) was chosen at a separation where the partners lie outside of one another's steric radii. The classical point charge–point induced dipole attraction at that distance is 3.7 kJ/mol, while the point charge–permanent dipole attraction is 6.8 kJ/mol. The B3LYP/6-31G** calculated attraction (electronic energy difference including counterpoise corrections for basis set superposition error) is 22 kJ/mol. Rotating the 4-pyridyloxy radical so that its permanent dipole repels the positive charge (making nitrogen the atom closest to the cation and keeping the center-of-charge to center-of-charge distance at 6.8 Å) is calculated to cost 14 kJ/mol at the B3LYP/6-31G** level, almost exactly equal to the classical prediction. We conclude that a classical model does not give a bad picture for the charge–permanent dipole interaction, but that the other contributions are greatly underestimated by a point charge–point induced dipole.

If a [cyclooctyl cation $^{\bullet}OC_5H_4N$] complex is allowed to collapse (subject to the constraint of $C_s$ symmetry) with the orientation shown in Scheme 7, the calculated distance between the bridging hydrogen and the oxygen shrinks to 4.5 Å and the bridging hydrogen–O–N angle is 172°. The classical point charge–point dipole attraction is 9.7 kJ/mol and the total B3LYP/6-31G** attractive potential is 40 kJ/mol. This structure has the highest energy of the four stable $C_s$ geometries having a bridged cyclooctyl

cation (all of which exhibit one imaginary vibrational frequency and will revert to the covalent radical cation if the symmetry constraint is removed). The zero point energy of the complex is 2 kJ/mol greater than that of the separated ion and neutral. Rotating the pyridyloxy ring 90° about the C–O bond (giving another structure with $C_s$ symmetry) permits the oxygen to approach 0.1 Å closer to the cyclooctyl cation, and the bridging hydrogen–O–N angle decreases slightly to 167°. The DFT-calculated attraction increases by 1 kJ/mol. If, instead, the cyclooctyl ring is flipped over (still maintaining $C_s$ symmetry) so that the bridging hydrogen is closest to the oxygen, the center-of-charge to center-of-charge distance between the two partners does not change, and the bridging hydrogen–O–N angle decreases to 164°. The DFT-calculated attraction increases to 46 kJ/mol. This structure has the lowest energy of the $C_s$ geometries.

As Scheme 7 depicts, the two hydrogens that are transferred end up on opposite ends of the pyridyloxy. This signifies that the ring must have rotated 180° in the course of the ion decomposition. Thus the experiment demonstrates that the reorientation criterion[30] has been fulfilled. The majority of cyclooctyl cations are formed in ion–neutral complexes because the photon energy is not high enough to yield free cations efficiently. Other mass spectrometric studies show that bond cleavages often favor the formation of carbocations within ion–neutral complexes, even when the internal energy greatly exceeds the threshold for producing free cations.[26]

Ion–neutral complexes have been called ''microscopic reaction 'vessels' '' for gas-phase ion chemistry.[36] They intervene in both unimolecular and bimolecular reactions and behave like gas-phase analogues of cage effects in solution.[37,38] Unimolecular heterolyses operate as gas-phase solvolyses to form complexes,[38,39] where the ion–neutral complex plays the same role as does an ion pair in solution. The lifetimes of ions within complexes are brief, and rearrangements take place in free ions that occur too slowly to be detected from the neutral products of complexes.

## III. PRODUCTS FROM TRITIUM DECAY

Nuclear decay transmutes one element into another. $\beta$-decay (the ejection of an electron from the nucleus) increases atomic number by 1 and imparts a positive charge to the remnant. This has proved a useful technique for creating gaseous cations under conditions where the neutral products of their ion–molecule reactions can be collected for analysis.[40–42] When the radionuclide is tritium, the net transformation is $^3H \rightarrow {}^3He^+$. When there

is more than one tritium in the starting material, the cation remains radioactive after one of the nuclei decays. Its radioactive neutral products can then be identified.

$$^{1}\mathrm{n}_0 \rightarrow ^{1}\mathbf{p}_1 + [\boldsymbol{W}^-] \tag{6}$$

$$[\boldsymbol{W}^-] \rightarrow \bar{\nu}_\mathrm{e} + \beta^- \tag{7}$$

$\beta$-decay is a three-body process, in which a neutron transforms to a proton. It can be viewed as a pair of successive two-body decays, summarized in equations 6 and 7. The first step (equation 6) is the decomposition to a pair of heavy particles, one of which is a virtual, negatively charged intermediate vector boson $\boldsymbol{W}^-$. This virtual particle has a lifetime $<10^{-25}$ s; hence, its mass can be very much larger than that of the original neutron. Decay of the virtual particle into an electron (the $\beta$-particle) and an antineutrino (equation 7) as a second step means that the angular distribution of the nuclear recoil is virtually independent of the direction of the $\beta$-particle. In other words, the momentum distribution of the antineutrino $\bar{\nu}_\mathrm{e}$ is essentially isotropic (if one neglects spin correlation effects, which are small). The average recoil energy of an $^3$He nucleus produced by $\beta$-decay of tritium is $<1$ eV, while the $\beta$-particle itself has an average kinetic energy on the order of 12 keV.[42]

$$\mathrm{R–T} \rightarrow \mathrm{R–He}^+ \rightarrow \mathrm{R}^+ + \mathrm{He} \tag{8}$$

$\beta$-decay converts a tritiated organic molecule, R–T, into a cation, as equation 8 illustrates. Some (but not all) of the molecular fragments attached to a disintegrating atom become internally excited following nuclear decay. Three general mechanisms dominate: (***a***) an ejected particle can collide with the rest of the molecule, possibly forming a superexcited state; (***b***) the molecular fragment can be left behind in a deformed geometry, which relaxes to an equilibrium structure containing a high degree of vibrational excitation; or (***c***) the molecular fragment is not left as equation 8 portrays, but rather as a multiply charged cation or as two or more smaller fragments. Mass spectrometric studies of the ions produced by tritiated organic molecules suggest the last option can often be neglected.[41,42] The first mechanism can produce ions that contain $>2$ eV internal energy, but the second mechanism produces ions containing $<2$ eV of internal energy.

Consider excitation mechanism (***a***) above. The arrows in Figure 1 represent a subset of the trajectories of ejected particles with their origin at a tritium nucleus attached to an $sp^3$ carbon. From the vantage point at the tritium nucleus, the rest of the molecule subtends a region of space easily contained within a 120° cone, which is represented by dashed lines. The odds

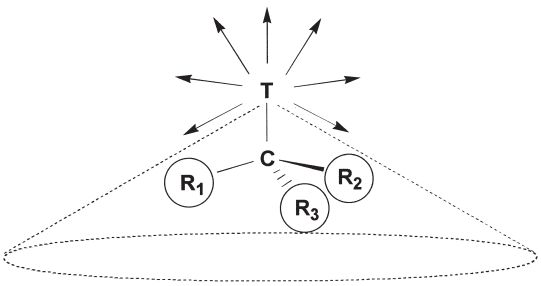


***Figure 1.*** Schematic representation of the directions of $\beta$-emission and 3He loss that do not lead to collision of ejected particles with the remaining carbocation (represented by arrows), as compared with the volume of space (represented by the dashed 120° cone) where such collisions are possible.

against the $\beta$-particle exiting within the cone are 3 : 1. Therefore the odds against the $^3$He atom exiting within the cone are also 3 : 1. We take the sum of the two probabilities as an upper bound for the net probability that one of the ejected particles collides with the carbocation from which it is departing. In other words, $\geq 50\%$ of the carbocations are formed without being struck by an ejected particle.

Now consider excitation pathway (***b***), vibrational excitation of carbocations that do not collide with a $\beta$-particle or a $^3$He atom. Of the total kinetic energy liberated by the nuclear decay (18.61 keV), an average of one-third is carried off by the neutrino (which does not interact with ordinary matter). Conservation of momentum dictates that, of the remaining kinetic energy, $<0.02\%$ is imparted to the $^3$He nucleus. The helium atom ought to carry off most of this recoil as translational kinetic energy when it detaches. The tritiated carbocation may be vibrationally excited, largely as a consequence of geometrical reorganization during departure of the helium.

$\beta$-emission takes place on the $10^{-18}$ s timescale. Therefore $^3$He forms in association with the $sp^3$ carbon to which tritium was attached. At this carbon–helium distance, $r_o$, the helium atom is repelled by the cationized carbon (even if it remains tetrahedral), since the equilibrium C–He distance is much longer than a C–H bond. If a nascent carbocation undergoes no geometrical relaxation, SCF calculations (including BSSE) give a repulsive potential of 25–30 kJ mol$^{-1}$ for expelling the helium atom. If the primary $sp^2$-cationic center is allowed to planarize, SCF calculations place the energy of the nascent cation on the order of 160 kJ mol$^{-1}$ above the final state. No potential energy barrier intervenes between the nascent cation and the final geometry, which has an SCF electronic

energy only 0.5 kJ below that of a free carbocation plus a helium atom. It is not clear whether the local minimum corresponds to a bound geometry, since the calculated zero point energy difference is comparable to the well depth.

Rehybridization should eject the helium atom as though from a slingshot, with coupling between the relaxation of the cation geometry and translation of the helium atom. It seems unlikely that all of the deformation energy is left in the carbocation when the $^3$He departs. The atom is accelerated to a velocity $v$ over a distance $r$ by the repulsive potential. If nuclear decay were to create an initially stationary helium atom, most of the relaxation energy would be carried away by the $^3$He as translational kinetic energy, $T_{He}$, as depicted by the lower curve in Figure 2. In that case, nearly all the potential energy would be converted to translational motion of the helium atom, and the atom could be accelerated to a final velocity as high as 13.5 $km\,s^{-1}$ relative to the cation. However, nuclear decay forms $^3$He with a high initial velocity, $v_o$. If the maximum possible recoil energy were wholly converted into $v_o$ of the helium atom (3.4 eV), the $^3$He would have an initial velocity $v_o \approx 15\ km\,s^{-1}$ in the center-of-mass frame. But because the neutrino typically carries off about one-third of the decay energy, the average tritium decay imparts an initial velocity on the order of $v_o = 10\ km\,s^{-1}$. As $v_o$ and $v$ have comparable magnitudes,

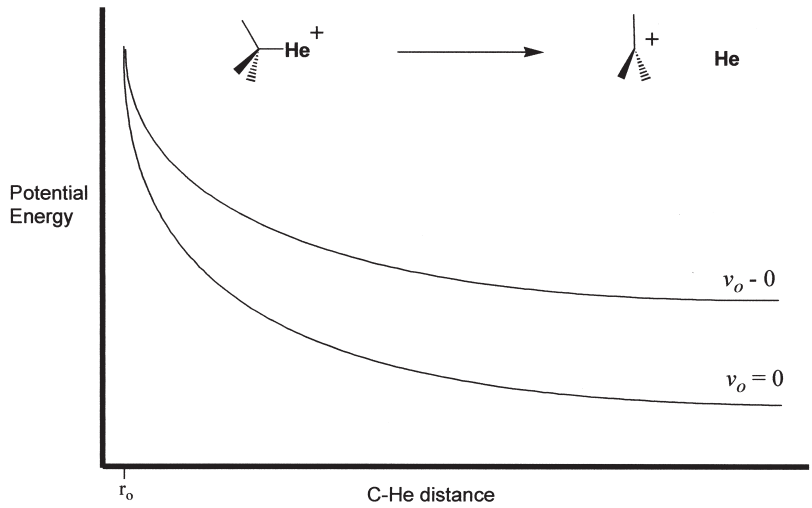


***Figure 2.*** Schematic picture of the conversion of strain energy into kinetic energy as a function of distance for an ejected He atom starting at rest at position $r_o$ (with velocity $v_o = 0$) versus one starting with initial velocity $v_o$.

the helium atom cannot be said to escape instantaneously from the carbocation.

$$T_{\mathrm{He}} = \int_{r_o}^{\infty} \frac{v}{v_o + v}\left(\frac{\mathrm{d}E}{\mathrm{d}r}\right)\mathrm{d}r \tag{9}$$

If $v_o$ were very much larger than $v$, the helium atom would be gone before the cation had time to rearrange at all. Nuclear decay of tritium bound to an $sp^3$ carbon represents a case intermediate between $v_o = 0$ and $v_o \gg v$. The helium atom is moving fast to begin with, so its outward motion is not strongly coupled to the geometrical relaxation of the cation. However, the shape of the repulsive potential curve does not exhibit a strong dependence on the direction the helium is travelling (so long as it is not within the dashed cone drawn in Figure 1). The force exerted on the helium atom, $\mathrm{d}E/\mathrm{d}r$, should exhibit the same dependence on the C–$^3$He distance, $r_o + r$, regardless of which of the solid arrows in Figure 1 comes closest to the direction of $v_o$. We derive equation 9 as a classical approximation for the relaxation energy carried off as $T_{\mathrm{He}}$ when $v_o \neq 0$ (in the limit where $T_{\mathrm{He}} = \Delta E$ when $v_o = 0$). Evaluation of SCF potential energy curves gives a value of $T_{\mathrm{He}}$ on the order of 110 kJ mol$^{-1}$ for a tritiated methyl group. In other words, the initial velocity $v_o$ of the $^3$He is fast enough to have gone before the cation has completely relaxed, carrying off only about 40% of the available relaxation energy. The partially relaxed cation structure that remains behind has a nearly planarized cation center.

Many experiments have been performed using tritium-containing ions derived from $\beta$-decay of multiply tritiated hydrocarbons.[42] Nuclear decay of tritiated methyl groups produces primary carbocations, which (unless they are conjugated with a double bond or cyclopropane ring) do not correspond to stable structures on their respective potential energy surfaces. Tritiated cations from *n*-alkanes rapidly transpose hydrogens to form secondary carbocations and, on a much slower timescale, undergo skeletal rearrangements to tertiary carbocations. The radiolabeled cations are captured by gaseous nucleophiles. The proportion of neutral products from secondary cations increases (and the proportion of tertiary cation products decreases) as the partial pressure of the nucleophile is raised.[42] A few percent of ostensible primary cation product has also been reported, probably from valence isomerization of primary cations to corner-protonated cyclopropanes.

Pertritiated methane (produced by the reaction of aluminum carbide with $T_2O$) yields tritiated methyl cations (symbolized as $CT_3^+$), whose gas phase chemistry has been extensively studied by Nefedov's group in Russia. One of their first major contributions was to provide evidence for methyl migration around protonated benzene rings, as summarized in Table 1.[43] In mixtures of xylenes (at their vapor pressure) and pertritiated methane,

***Table 1.*** Radiochemical vields of Trimethylbenzenes from Reaction of Xylenes with $CT_4$. Numbers in Parentheses Indicate Statistical Proportions

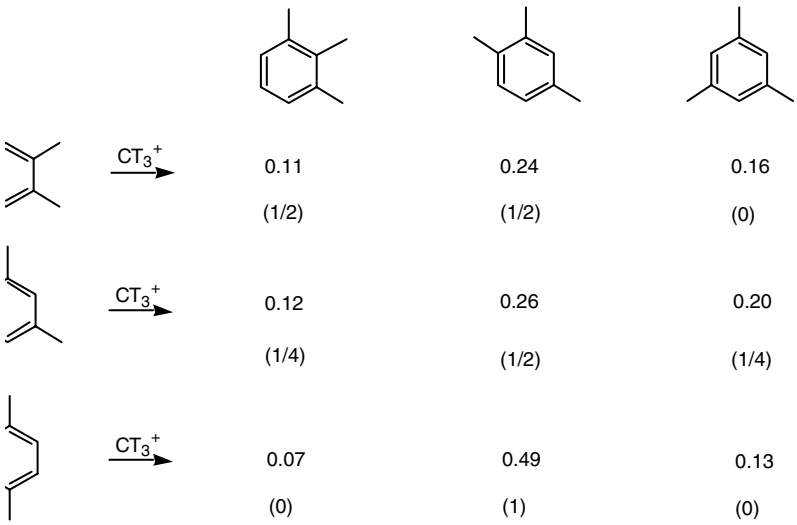


all three trimethylbenzenes are recovered as radiolabeled neutral products. In Table 1, the fractions in parentheses represent the statistical proportions of the methylation products that would be expected if methyl groups could not transpose (calculated using the algorithm outlined in Section II.B above). As is apparent from the experimental yields, the different xylene isomers afford different proportions of products, signifying that complete equilibration does not take place during the lifetime of the ion. These experimental results present one of the earliest demonstrations of orbital symmetry-allowed suprafacial sigmatropic shifts of methyl groups.

Another test of orbital symmetry comes from the reaction of methyl cations with ketones. ICR experiments have shown at least 10 different pathways for reaction of $CD_3^+$ with acetone. One of the minor pathways produces $C_3H_5^+$ cation.[44] Thermodynamically it is plausible that the neutral products are formaldehyde and molecular hydrogen, as equation 10 depicts for the orbital-symmetry allowed decomposition of the

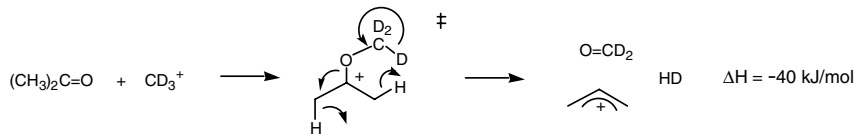


(10)

vibrationally excited adduct ion (the overall ion–molecule reaction would still be about 20 kJ/mol exothermic if the product ion has the $CH_3C{=}CH_2^+$ structure instead of the more stable allyl cation). However, a systematic study of the neutral products from $CT_3^+$ on a variety of gaseous ketones (analyzed by gas chromatography with a radioactivity detector) showed that the major tritiated neutral product is methanol rather than formaldehyde.[45]

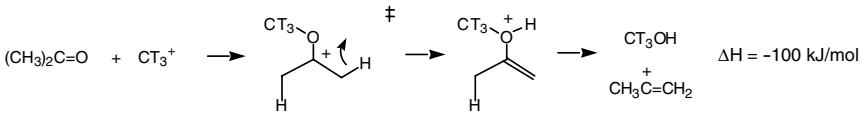


(11)

Assuming that the principal product is $CT_3OH$, Speranza has proposed the isomerization of the vibrationally excited adduct ion via a concerted, unimolecular 1,3-hydrogen shift, as equation 11 portrays.[42] Orbital symmetry forbids this as a suprafacial isomerization. The question has lately been posed, whether planar, even-electron gaseous ions of this sort rearrange antarafacially.[46] If so, the molecular skeleton ought to retain its plane of symmetry in the transition state, and the migrating hydrogen should pass through that plane, as drawn to the left in Scheme 8.

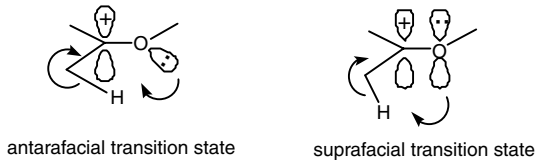


***Scheme 8.***

Oxygen has two lone pairs, and Scheme 8 contrasts two possible transition states. In the thermally forbidden suprafacial transition state (to the right), the itinerant hydrogen moves onto the lone pair that is parallel to the vacant p-orbital of the cation. The molecular skeleton can become nonplanar (e.g. by twisting about the $sp^2$ carbon–oxygen bond), and C=O double bond character can be sacrificed to increase the double bond character of the newly forming C=C double bond. By contrast, the antarafacial transition state transfers hydrogen to the other oxygen lone pair, which lies in the molecular plane. The C=C double bond develops

in a highly twisted geometry. The question remains open whether the distortion required for the symmetry-allowed antarafacial transition state destabilizes it to such an extent that the suprafacial one is lower in energy.

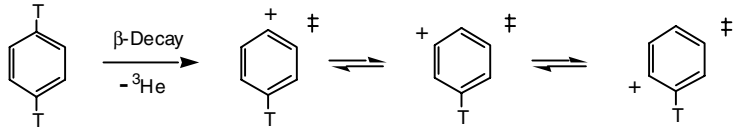


(12)

Researchers in Rome have examined many other multiply tritiated hydrocarbons. This body of work includes comprehensive studies of the phenyl cation produced by the $\beta$-decay in equation 12. The phenyl cation is difficult to prepare in condensed media but forms directly from $\beta$-decay of tritiated benzene. Its neutral reaction products in the gas phase have been carefully probed by a number of well-controlled experiments. An elegant series of investigations has demonstrated that intramolecular hydrogen migration within the vibrationally excited cation occurs on the 10–100 ns timescale, as equation 12 depicts (despite initial theoretical predictions that this isomerization should have a barrier too high to permit this).[42] Methylated phenyl cations rapidly transpose ring hydrogens, too, without detectable isomerization to the much more stable benzyl cation. The proportions of neutral methylanisoles summarized in equation 13 have been observed by capture of the cation with methanol and are probably not far from representing the equilibrium distribution of isomeric ions.[47] The bimolecular reactivity of other monosubstituted substituted phenyl cations $XC_6H_3T^+$ (X = F, Cl, Br, $NO_2$, $OCH_3$, and CN) has also been reported.[48]

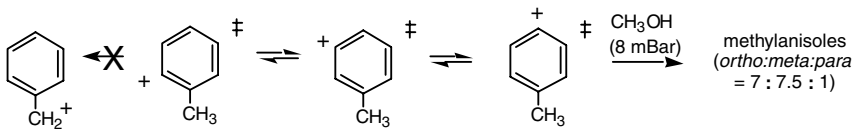


(13)

Capture of phenyl cations with methyl *n*-propyl ether gives products in which rearrangement has taken place.[49] Initial capture gives the oxonium ion drawn to the left in equation 14. Most of this ion eliminates propene, and deprotonation of the resulting ion affords anisole (PhOR, where R = methyl), which constitutes 75% of the radiochemical yield. Among the other products are isopropyl phenyl ether (roughly 3% of the radiochemical yield, about 3 times more abundant than *n*-propyl

phenyl ether) and the isopropyl anisoles (also roughly 3% of the radiochemical yield).

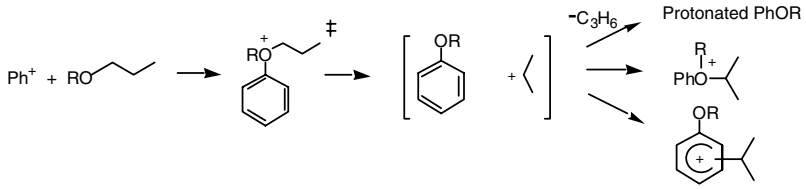


(14)

The most economical explanation supposes that the initially formed adduct of $Ph^+$ with an *n*-propoxy group, $PhO(R)CH_2CH_2CH_3^+$, behaves the same way as does protonated *n*-propyl phenyl ether (R=H), whose rearrangements have been examined using mass spectrometry of a number of specificially deuterated analogues.[50–53] The protonated ion decomposes via propene loss. The mass spectrometric studies also reveal that the hydrogens of the *n*-propyl group randomize and that they exchange with the hydrogen initially bound to oxygen (but not with the ring hydrogens). The intermediacy of the [PhOR $(CH_3)_2CH^+$] ion–neutral complexes accounts for the results. These complexes interconvert (but do not equilibrate completely) with [$PhO(H)R^+$ $CH_3CH{=}CH_2$] complexes. Kinetic analysis of the ion intensity ratios from protonated *n*-propyl phenyl ethers (analogous to that described in Section II.C above) shows that interconversion of the covalent oxonium ion with the latter complex cannot, by itself, account for the deuterium labeling data measured by mass spectrometry.[51]

Another mass spectrometric experiment from this laboratory (P.S. Mayer and T.H. Morton, unpublished results) confirms the pathway for decomposition of the covalent oxonium ion shown for $R{=}C_2H_5$.
Chemical ionization of *n*-propyl phenyl ether with methane reagent gas at 0.0001 mbar produces a substantial peak corresponding to an adduct with ethyl cation. This adduct ion decomposes extensively via propene expulsion to give protonated $PhOC_2H_5$ (*m*/*z* 123). When deuterated *n*-propyl phenyl ethers are chemically ionized in this fashion, both *m*/*z* 123 and *m*/*z* 124 form. In the chemical ionization source $PhOCH_2CH_2CHD_2$ gives an *m*/*z* 123 : *m*/*z* 124 intensity ratio of 2.4 : 1; $PhOCD_2CH_2CH_3$ gives a ratio of 2.85 : 1; $PhOCH_2CH_2CD_3$ gives a ratio of 1.5 : 1; and $PhOCD_2CD_2CH_3$ gives a ratio of 1.15 : 1. Intermediacy of ion–neutral complexes such as drawn predicts this sort of result, in which the transferred hydron can come from every position of the propyl chain.

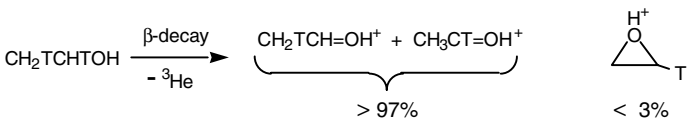


(15)

A few experiments have been performed on multiply tritiated molecules containing functional groups. Tritiated ethanol, in which the principal isotopomer is $CH_2TCHTOH$, has been permitted to undergo $\beta$-decay in the presence of 0.5 bar of gaseous trimethylamine. At that pressure the ion-molecule collision rate is faster than $10^{10}$ $s^{-1}$. The recovered radioactive neutral product is predominantly acetaldehyde, with a barely detectable yield of ethylene oxide (in a ratio $\geq 40:1$). As equation 15 summarizes, this implies that nuclear decay produces, for the most part, protonated acetaldehyde, regardless of which tritium expels a $\beta$-particle.[52]

Since the two tritium atoms are equally likely to decay, one would expect half of the initially formed ions to have the nascent primary cation structure $HOCHTCH_2^+$. Yet very little of the recovered neutral product comes from protonated ethylene oxide. Two possible explanations may be advanced to account for this. One is that hydride shift is much more favorable than oxygen bridging, even though oxygen bridging is calculated to have no energy barrier. The alternative explanation holds that protonated ethylene oxide does form, but with such high vibrational energy that it rearranges completely on the $10^{-10}$ s timescale before deprotonation by collision with trimethylamine.

One test of the latter hypothesis involves preparing a higher homologue, whose isomerization ought to yield characteristic products. To that end, the ditritiated *n*-propanol shown in Scheme 9 was synthesized and the neutral products from its $\beta$-decay analyzed. Decay of the tritium at position 3 yields tritiated ethylene by cleavage of a carbon–carbon bond. Both propylene oxide and propionaldehyde are recovered as tritiated products from decay at position 2 in the presence of 0.5 bar trimethylamine, but no acetone is seen.[55] Protonated acetone would be expected among the thermal rearrangement products of protonated propylene oxide. The absence of acetone among the neutral products indicates that protonated epoxides

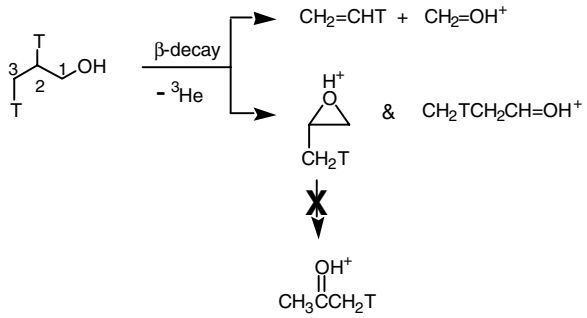


***Scheme 9.***

formed by oxygen bridging are stable on the $10^{-10}$ s timescale. Therefore the low yield of ethylene oxide from ditritiated ethanol must reflect a preference for hydride shift versus oxygen bridging. Mass spectrometric studies of unimolecularly generated [$CH_4D_2O^+$ $PhO^\bullet$] ion–neutral complexes confirm this inference.[54]

## IV. PRODUCTS FROM RADIOLYSIS EXPERIMENTS

Various forms of radiation have been used to produce ions in sufficient quantitites to yield neutral products for subsequent analysis. In principle, it should be possible to use intense beams of UV below ionization threshold for this purpose. To date, however, efforts to collect neutrals from resonant multiphoton ionization (REMPI) have not succeeded. In one experiment, 1 mbar of gaseous *n*-propyl phenyl ether was irradiated at room temperature with a 0.1 W beam of 266 nm ultraviolet (from an 800 Hz laser that gives 8 n pulses) concurrent with a 0.5 W beam at 532 nm.[56] The beams were intense enough not only to ionize the ether in the mass spectrometer, but also to excite it so that it expels propene.[26] After several hours of irradiation $<10\%$ of the starting material remained. Production of carbon monoxide and acetylene (decomposition products of the phenoxy group) could be detected by infrared absorption spectroscopy, but the yield of neutral propene (as measured by NMR spectroscopy) was infinitesimal.

This outcome illustrates one of the obstacles confronting the analysis of neutral products. Ion detection has such high sensitivity that REMPI can be effective in a mass spectrometric experiment even if it produces $<10$ ions per laser pulse. The techniques for examining neutrals (e.g. GC-MS or NMR) provide structural information that ion studies cannot accomplish, but they require much greater amounts of product. In order to observe uncharged dissociation products directly, REMPI would have to produce $>10^8$ ions per laser pulse.

Ionizing radiation ($\gamma$-radiolysis[57–59], vacuum ultraviolet,[60] electron impact[18,61]) has been the method of choice for neutral product collection studies under a variety of experimental conditions. On one hand, irradiations with $\gamma$-rays or vacuum ultraviolet are typically performed on static samples at pressures $>1$ mbar. On the other hand, electron beams with energies $<100$ eV are hard to sustain at pressures $>0.001$ mbar. Electron impact experiments are run on flowing samples at low pressure, which reproduces the conditions found in many ordinary mass spectrometers. Neutral product studies have provided the best measure of the scope and limitations of the two categories of cation rearrangement—ring closure/ring opening and atom/group transfer—listed in the opening

paragraph of this chapter. The first category comprises ring closure and its reverse reaction, ring opening.

## A. Ring Closure/Ring Opening

Equation 16 illustrates a celebrated example where ring closure competes with vicinal hydride shift (a common form of atom transfer in cations, which does not take place in free radicals or anions). The gas phase reaction was explored by preparing the dimethylfluoronium ion, $(CH_3)_2F^+$, by $\gamma$-radiolysis of fluoromethane. Exothermic methylation of a sample of $^{13}C$-$\beta$-phenethyl chloride (where the asterisk in equation 16 symbolizes the labeled position) in the gas mixture gives a vibrationally excited ion that loses chloromethane to form two isomeric ions, $\alpha$-phenethyl cation and spirooctadienyl cation (sometimes called ethylenebenzenium). Nucleophilic attack by methanol in the reaction mixture yields $PhCH(CH_3)OCH_3$, whose isotopic label remains almost entirely at the methyl group. The recovered $PhCH_2CH_2OCH_3$ contains $^{13}C$ equally distributed between the two methylene positions.[62] The spirooctadienyl ion does not isomerize to $\alpha$-phenethyl cation, even though DFT calculations predict the latter to be 55 kJ/mol more stable.

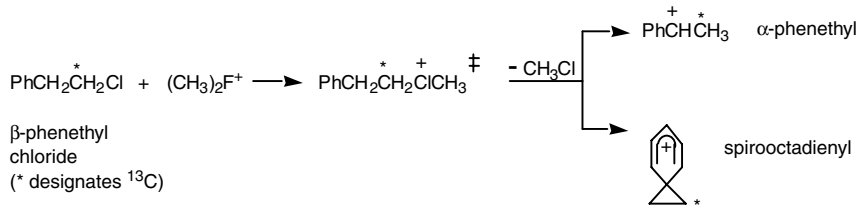


(16)

Nucleophilic capture of the spirooctadienyl cation opens the 3-member ring. This behavior characterizes many reactions of many other cyclopropane-containing carbocations, as well. $\gamma$-radiolysis of perdeuterated propane forms $C_3D_7^+$ ions, most of which either transfer $D^+$ or form isopropyl adducts. As the propane pressure is raised from 1000 mbar to 2000 mbar, however, the isopropyl/*n*-propyl adduct ratio falls from 30 : 1 to about 5.5 : 1.[63] This implies the formation of corner-protonated cyclopropane, which reacts with nucleophiles as though it were an *n*-propyl cation. With increased pressure, vibrationally excited protonated cyclopropane experiences more frequent nonreactive collisions, which deactivate it and slow down its rate of unimolecular isomerization to isopropyl cation.

Cationic cyclization and its reverse have particular relevance, since ring closure and ring opening have been invoked to account for a large number of biosynthetic pathways.[1,2] The gaseous cyclopropylcarbinyl–cyclobutyl–homoallyl system represents an extreme instance of a rapid, reversible isomerization of this sort, which has been studied over a period of 20 years both by $\beta$-decay of tritiated cyclobutane[64] and by radiolytic methods.[65] This interconversion is so fast that the three $C_4H_7^+$ structures have been discussed as resonance forms of a nonclassical ion. In any event, their energies are so close and the barriers among them (if they exist at all) are so low that medium and counterion effects very likely influence whether $C_4H_7^+$ is an equilibrating system or not.

Carbocations that contain small rings display a range of unimolecular reactivity, in the sense that some do not rearrange to more stable isomers (such as the spirooctadienyl cation in equation 16); some isomerize at measurable rates (such as corner-protonated cyclopropanes); and some exhibit very rapid interconversion (such as cyclopropylcarbinyl–cyclobutyl–homoallyl). What happens with larger rings? $\beta$-decay experiments on tritiated cyclopentane in the presence of unlabeled cyclopentane show a measurable yield of radioactive 1-pentene (and complete absence of 2-pentene), suggesting that cyclopentyl cation can undergo ring opening.[66] Since $CH_2{=}CHCH_2CH_2CH_2^+$ does not correspond to a stable structure on the $C_5H_9^+$ potential energy surface, the sequence summarized in equation 17 seems likely to be taking place. DFT calculations portray the 4-penten-2-yl cation as a resonance hybrid with the 2-methylcyclopropylcarbinyl cation, as drawn. The second step of equation 17, quenching $CH_2{=}CHCH_2CHCH_3^+$ by hydride transfer from neutral cyclopentane, is endothermic and is probably driven by residual vibration excitation in the pentenyl cation.

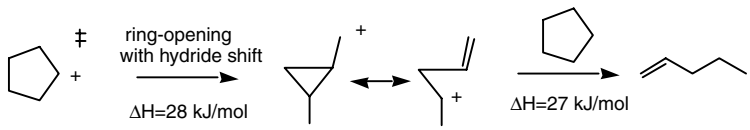


(17)

Ring closure of nascent $CH_2{=}CHCH_2CH_2CH_2^+$ within ion–neutral complexes has been studied using a specially designed Electron Bombardment Flow (EBFlow) reactor, schematically drawn in Figure 3. This apparatus has the advantage that the conditions under which ions are formed and react (70 eV electron impact; pressure $\leq 0.001$ mbar) closely parallel those in mass spectrometer sources. The neutral product yields are routinely interpreted with reference to the ionic products observed by the mass spectrometry. Hypotheses based on EBFlow results for ion–neutral complexes are further tested by comparison with mass spectrometry.

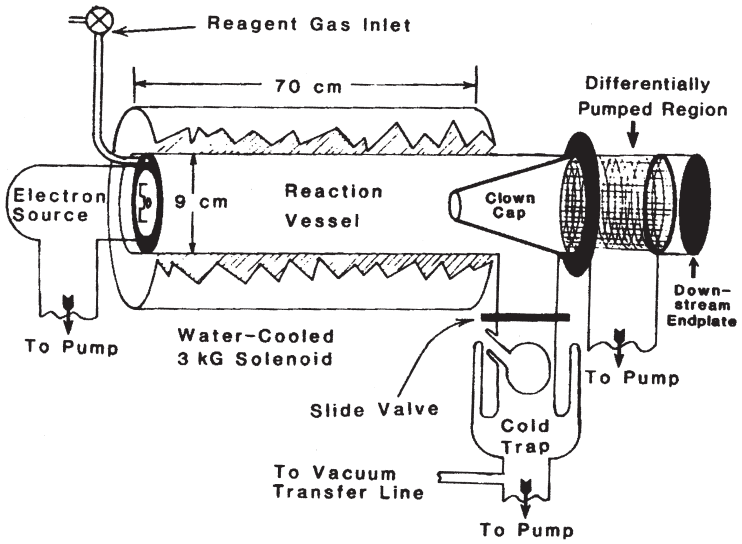


***Figure 3.*** Schematic of an Electron Bombardment Flow (EBFlow) reactor. The magnetic field maintains the electron beam along the axis of the solenoid. The beam's negative charge prevents cations from migrating to the walls, and all charged species are dumped into the differentially pumped region downstream of the clown cap, where they are pumped away and do not contaminate the neutrals collected in the cold trap, which come from the EBFlow reaction vessel.

The cylindrical EBFlow reaction vessel is modeled on a conventional electron ionization (EI) source, but with the path of electron beam enlarged by a factor of 1000. An external solenoid electromagnet keeps the electrons on the cylinder axis, and the space-charge of the beam (along with the magnetic field) prevents collisions from driving ions to the walls. At the far end of the vessel, electrons and ions exit to a differentially pumped chamber via a conical Faraday plate (''clown cap''), while neutrals find their way into a liquid nitrogen-cooled trap, where they are collected.[18] Keeping ions off the walls is important, since surface neutralization can produce the same sorts of products as homogeneous gas-phase reactions (this has previously been discussed with regard to an earlier EBFlow design[15]). Efficiency of neutral product collection has been estimated to be on the order of 85%.[18] EBFlow yields are normalized relative to the beam current and expressed in units of μmole per ampere-second (i.e. per coulomb) of incident electrons, a μmol/A-s. A yield of 1 molecule per electron corresponds to 10.36 μmol/A-s. Given typical cross sections for 70 eV electron ionization, a pathlength on the order of 1 metre, and a

reactant pressure of 0.005 mbar, theoretical yields should be on the order of 2–3 μmol/A-s.[18]

The electron beam produces free radicals as well as cations. Neutral radicals tend not to isomerize (or, if they do, they rearrange by pathways different from those of cations). As a result, the neutral products from cationic rearrangements can generally be distinguished from the ones that arise via neutral free radicals. To judge from the relative abundances of neutral products recovered from the EBFlow, 70 eV electron impact produces more cations than radical pairs. Only very light hydrocarbons (e.g. ethylene and acetylene) are formed in yields comparable to the yields of cationic products.

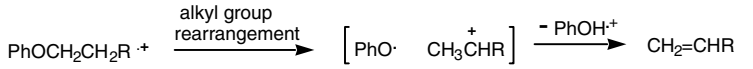


(18)

One major focus of study has been the neutral products from 70 eV electron bombardment of primary phenoxyalkanes of the general formula $PhOCH_2CH_2R$. Unlike secondary alkyl phenyl ethers (whose radical cations expel alkenes via *syn*-elimination, as exemplified by Schemes 1 and 4), primary alkyl phenyl ether molecular ions decompose by formation of ion–neutral complexes via bond heterolysis accompanied by alkyl group rearrangements, such as equation 18 illustrates[13,26–29,61,67]. The corresponding neutral products are typically alkenes, which have been collected in the EBFlow and subsequently analyzed by chromatographic or spectroscopic means.[18,34,61,68–73] In all cases, vicinal hydride shift (as in equation 18) takes place. With alkyl groups having more than two methylenes, hydride shifts can continue down the chain. The question arises as to what other reactions compete with equation 18.

EBFlow radiolyses of 1-phenoxyalkenes of the general formula $PhOCH_2(CH_2)_nCH{=}CH_2$ give measurable yields of cycloalkenes, signaling that the ring closure represented in Scheme 10 competes with hydride shift. Internal nucleophilic displacement of phenoxy radical by the double bond leads to ion–neutral complexes containing cycloalkyl cations. Bond homolysis is ruled out by the fact that 4-penten-1-yl radicals do not cyclize,[74] as well as by the virtual absence of methylenecyclopentane among

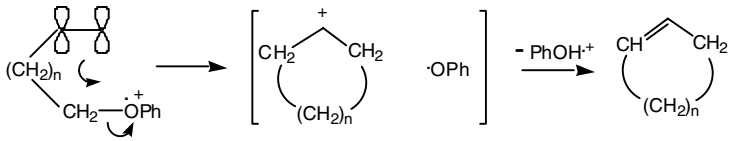


***Scheme 10.***

the products for $n=3$ (which would be the cycloalkene expected to result from intramolecular cyclization of 5-hexen-1-yl radicals[74]). Previously published GC traces display the product distributions for $n=2$ and 3.[18] For $n=2$ the yield of cyclopentene from Scheme 10 is 0.2 μmol/A-s, while the yield of linear pentadienes from hydride shift is about 10 times greater. The 1,3-pentadienes (which must have come from 1,2-hydride shifts) constitute >60% of the $C_5H_8$ neutral products, 1.5 μmol/A-s in a *trans*/*cis* ratio of 2.4 : 1. Skeletal rearrangement to the most stable allylic cation gives isoprene as a neutral product in a low yield (0.03 μmol/A-s), which probably comes about in the small amount of free $C_5H_9^+$ produced by 70 eV electron impact on $PhOCH_2CH_2CH_2CH{=}CH_2$. As mentioned above, mass spectrometric studies complement EBFlow experiments. The proportion of $PhOD^{\bullet+}$ seen in the 70 eV mass spectrum of $PhOCH_2CH_2CH_2CH{=}CD_2$ is in accordance with the yield of cyclopentene in the EBFlow.

Cyclization to form 6-membered rings competes more favorably with hydride shift. Linear hexadienes with terminal $CH_2$-groups (expected products of equation 18) are recovered in a yield of 0.6 μmol/A-s for the case $n=3$, while cyclohexene constitutes a yield of 0.35 μmol/A-s; 1-methylcyclopentene 0.08 μmol/A-s; and the other methylcyclopentenes 0.06 μmol/A-s. Products characteristic of free $C_6H_{11}^+$ cations that rearrange to the most stable allylic structures—2,4-hexadienes and branched $C_6H_{10}$ dienes—are recovered in a yield of 0.15 μmol/A-s. As in the $n=2$ case, the products from cations produced in ion–neutral complexes greatly exceed those from free cations produced by simple bond fission, just as the 70 eV mass spectrum would predict.

EBFlow experiments also provide evidence for ring closure to form a 7-membered ring, but products from other cyclizations are more abundant. Unfortunately, there are so many $C_7H_{12}$ isomers that it is difficult to separate them all by gas chromatography. Cycloheptene stands well apart, though, and is recovered in a yield of 0.02 μmol/A-s, as compared to a yield of 0.05 μmol/A-s for 1-methylcyclohexene and 0.05 μmol/A-s for other methylcyclohexenes and ethylcyclopentenes (which presumably arise via ring closures that take place after the hydride shift). Linear dienes from hydride shifts are recovered in a yield of 0.25 μmol/A-s.

Comparing cyclization yields with those of linear dienes with terminal $CH_2$-groups gives a measure of the dependence of Scheme 10 on chainlength. Closure to a 6-membered ring ($n=3$) goes 0.6 times as fast as vicinal hydride shift, while closure to a 5-membered ring ($n=2$) goes 0.1 times as fast and closure to a 7-membered ring goes only 0.07 times as fast. This outcome can be compared with the low probability of forming an epoxide in equation 15. However, other cationic cyclizations give a higher probability of 3-member ring formation than does equation 15.

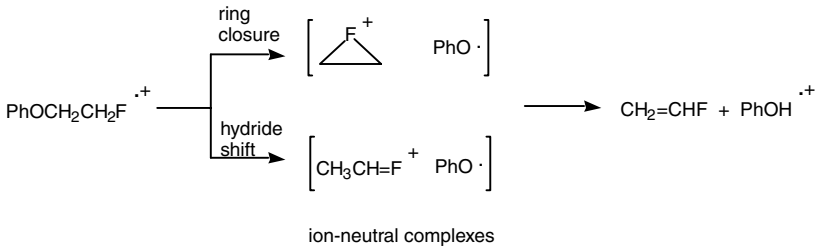


(19)

Cyclic, 3-member halonium ions are well-known intermediates for chlorine, bromine, and iodine. The question as to whether cyclic fluoronium ions might exist as stable entities was decided by an EBFlow experiment that generated them in ion–neutral complexes. As in the case of ring closure to the spirooctadienyl cation (equation 16), ring closure takes place in competition with hydride shift. Ionized $\beta$-fluorophenetole dissociates via two competing pathways, as equation 19 represents, which would be indistinguishable in the absence of isotopic labeling. Both involve heterolysis of the $sp^3$-carbon oxygen. The upper pathway drawn has the fluorine bridging between two carbons, yielding a symmetrical epifluoronium ion. The hydride shift in the lower pathway forms the most stable of the possible $C_2H_5F^+$ structures. The two competing mechanisms operate in about a 1 : 2 ratio (hydride shift favored), as revealed by $^{19}F$ NMR of the neutral fluoroethylenes from $PhOCH_2CD_2F$ and $PhOCD_2CH_2F$.[70] The upper pathway yields $CH_2{=}CDF$ and $CD_2{=}CHF$ regardless of which isomer is ionized. The lower pathway yields different products from the isomeric dideuterated starting materials, as Scheme 11 summarizes.

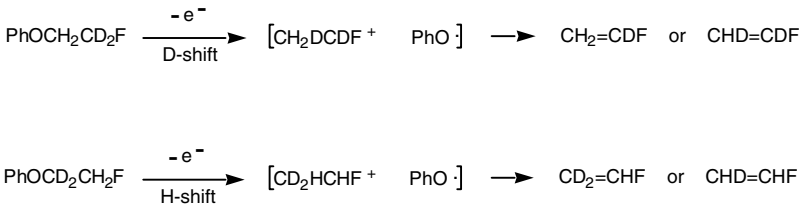


***Scheme 11.***

Consider three possibilities. If only hydride shift occurs, just the products shown in Scheme 11 will be detected. If, by contrast, bridging is followed by hydride shift, the EBFlow will recover all four possible deuterated fluoroethylenes from either starting material (although not necessarily in identical proportions). Finally, if (as in equation 16) bridging and hydride shift represent separate pathways that produce noninterconverting

intermediates, each starting material will afford only three products (neglecting *cis-trans* isomerism). This last outcome has been observed. On the one hand, no CHD=CDF is recovered from $PhOCD_2CH_2F$, and no CHD=CHF is recovered from $PhOCH_2CD_2F$. On the other hand, the observation of $CH_2$=CDF from $PhOCD_2CH_2F$ and $CD_2$=CHF from $PhOCH_2CD_2F$ provides the first unequivocal evidence for an epifluoronium ion.[70]

## B. Atom/Group Transfer

The evidence for cyclization presented in the previous section raises a series of questions. From a topological standpoint, any transfer of an atom/group from one position to another either passes through a cyclic structure or else involves a bond cleavage followed by recombination. How can one tell the difference? If an atom/group transfer involves a cyclic structure, does it operate via reversible ring closure/ring opening sequences? Or does the cyclic structure simply represent a transition state? Questions of this nature have intrigued mechanistic chemists for many years. Before attempting to address them, a survey of vicinal atom/group transfer will illustrate the scope of this process beyond the hydride transfer represented by equation 18.

Scheme 12 summarizes a $\gamma$-radiolysis performed on a mixture of benzene-$d_6$, $CF_4$, and ethylene. Ionization of $CF_4$ yields $CF_3^+$, which has been called an "ionic Lewis superacid."[75–77] Electrophilic attack on benzene-$d_6$ gives the conjugate acid of perdeuterated trifluorotoluene, $CF_3C_6D_6^+$, as the first step of Scheme 12. Trifluorotoluene is more basic than ethylene; hence, the ion–molecule reaction of $CF_3C_6D_6^+$ with ethylene cannot give a Brønsted acid–base reaction. The only thermochemically accessible pathway to ethyl trifluorotoluenes is via ion–neutral complexes containing the ethyl cation

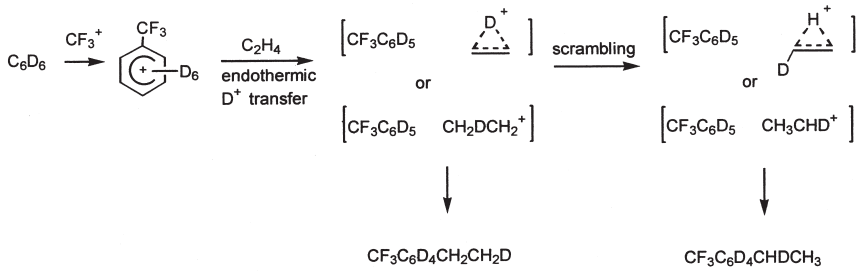


***Scheme 12.***

and neutral trifluorotoluene. Within the ion–neutral complexes, a small fraction (in the range of 7–9%, depending on the temperature of the reaction mixture) of the ethyl cations appear to scramble label.[78]

Theory suggests that the ethyl cation has a nonclassical equilibrium geometry with a proton sitting in the middle of a double bond (the dashed-line structures in Scheme 12), but the interpretation of the results does not depend on whether the cation prefers a classical or nonclassical geometry. Scheme 12 represents both alternatives. Recovery of products with undeuterated methyl groups means that classical structures have been accessed, either as a transition state in passing from a $D^+$-bridged to a $H^+$-bridged geometry or as the preferred structure in the complex, which undergoes a vicinal hydride shift. The competition between scrambling and formation of the final products means that if the rate of scrambling is known, then the average lifetime of the ion–neutral complex can be deduced.[78]

Vicinal shifts occur not only in cations, but also in neutral reactants that are in the process of acquiring a positive charge. The hydride abstraction by *tert*-butyl cation depicted in Scheme 13 has not been observed by ICR[79] nor in radiolysis experiments at pressures $<200$ mbar.[57] But $\gamma$-radiolysis at higher pressures permits noncovalent clustering to form encounter complexes, in which the ion and neutral have time to adopt the right geometry for methyl migration to occur simultaneously with bimolecular hydride abstraction, as the curved arrows show. The transition state is thought to require *anti*-periplanar disposition of the reacting bonds. The entropic barrier for this concerted reaction apparently requires thermal activation of the encounter complex, even at the expense of collisionally dissipating the energy liberated by clustering. In the presence of added methanol the final product is the methyl ether drawn at the bottom of Scheme 13.[79]

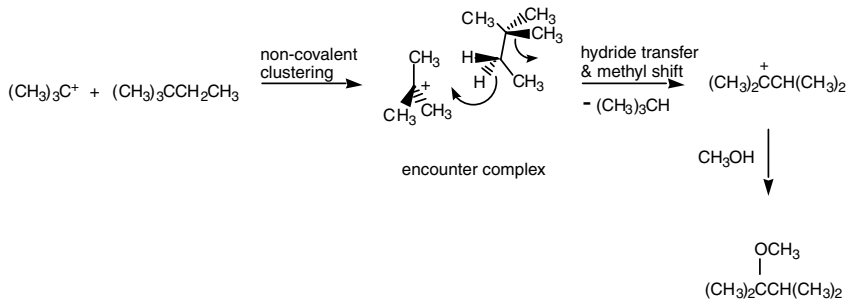


***Scheme 13.***

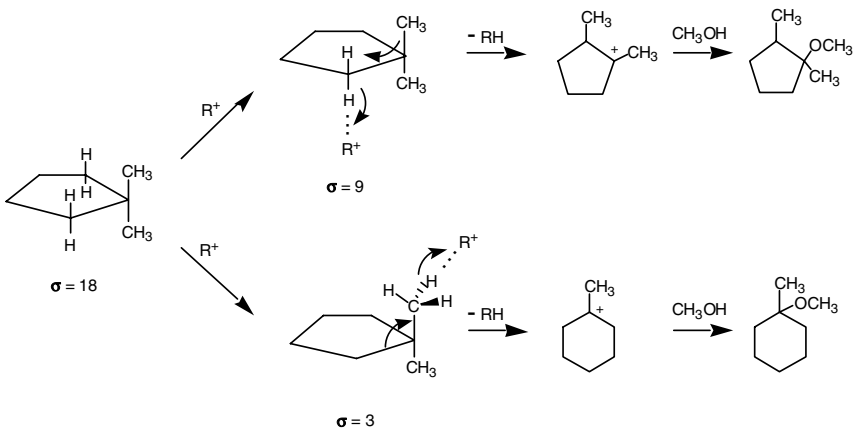


***Scheme 14.***

Neutral product distributions also measure the competition between the carbon–carbon bond shifts when a hydride is abstracted from 1,1-dimethylcyclopentane, as represented in Scheme 14. A radiolytically generated alkyl cation ($R^+$) can abstract from the ring (upper pathway) or from a methyl (lower pathway). As the symmetry numbers indicate, the lower pathway is favored on the basis of reaction path degeneracy. Also, according to DFT calculations, the methylcyclohexyl cation in the lower pathway is 1 kJ/mol more stable than the, dimethylcyclopentyl cation in the upper pathway. Nevertheless, in the presence of added methanol the corresponding methyl ethers are recovered in a 92 : 8 ratio in favor of the upper pathway when $R^+ = (CH_3)_3C^+$.[80] The *cis* and *trans* isomers from the upper pathway are recovered in virtually equal quantities, which tends to argue against the products coming from a terbody complex of $R^+$, methanol, and 1,1-dimethylcyclopentane. The lower pathway becomes more prominent as $R^+$ becomes more electrophilic, as would be expected from the reactivity–selectivity principle: the proportion of methylcyclohexyl ether roughly doubles when $R^+$ is the isopropyl cation.

Shifts of different atoms/groups to the same cationic center provide a measure of relative propensities to migrate. Three ion–neutral complexes form from the molecular ion drawn in Scheme 15. The EBFlow experiment required two isotopic labels (the asterisk designates $^{13}C$) in order to tease apart the different pathways (including about 10% of the molecular ions that eliminate $PhOD^{\bullet+}$ via *syn*-elimination to yield undeuterated 2-fluoropropene). Product analysis was rendered more difficult because the two 1-fluoropropyl cations $CH_3CH_2CHF^+$ and $CH_3CHCH_2F^+$ have nearly the

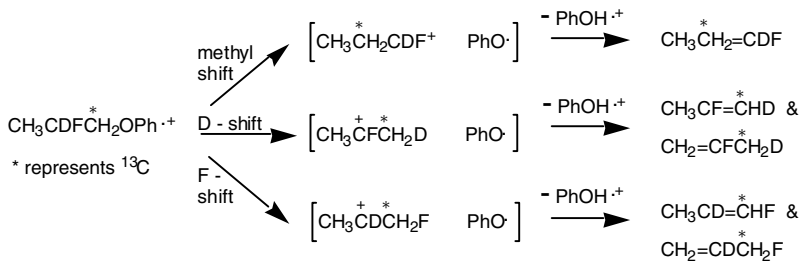


***Scheme 15.***

same stability and interconvert rapidly, scrambling (but not completely equilibrating) the deuterium label. $^{19}$F NMR resolves five different isotopomeric/isomeric *Z*-1-fluoropropenes (as well as five *E*-1-fluoropropenes), permitting a quantitative assessment of migratory aptitudes—methyl shift : D-shift : F-shift = 6 : 11 : 2.[69]

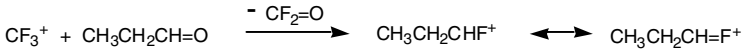


(20)

The predominance of methyl and D-shift reflects the fact that a fluorine substituent attached to an $sp^2$-cation center exerts a stabilizing influence due to delocalization of a fluorine lone pair onto the electron-deficient carbon (as exemplified by the resonance structure at the right in equation 20). This effect is well attested and has been used to guide the regiochemistry of cationic organic syntheses.[81,82] The 1-fluoroisopropyl cation from F-shift in Scheme 15 does not enjoy this effect, since fluorine is attached to an $sp^3$-carbon instead. Although it is a secondary carbocation, the electronegativity of the vicinal fluorine destabilizes it, even as fluorine stabilizes the primary carbocation produced by methyl shift. For these reasons $CH_3CH_2CHF^+$ and $CH_3CHCH_2F^+$ have nearly the same stability.

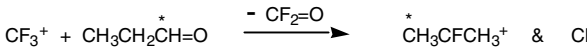


(21)

Free fluoroalkyl cations are produced by metathesis of perfluoroalkyl cations with simple carbonyl compounds.[83,84] Bimolecular exchange of $F^+$ for O between $CF_3^+$ and acetone forms $(CH_3)_2CF^+$, which is the most stable structure on the $C_3H_6F^+$ potential energy surface.[69] A variety of gas phase reactions create that ion. Neutral products can be recovered in the EBFlow from its gas phase ion–molecule reactions: $CH_3CF{=}CH_2$ from proton transfer to neutral acetone, for example, or $(CH_3)_2CF_2$ produced by fluoride

abstraction from *tert*-butyl fluoride.[85] $CH_3CFCD_3^+$ affords neutral products that have not transposed label between the two methyls (i.e. no products with partially deuterated methyl groups are seen).[86] Even when the ion has enough internal energy to expel HF unimolecularly, the neutral products from the resulting 2-propenyl ion exhibit no evidence for having scrambled hydrogens prior to its neutralization.[87]

When propionaldehyde reacts with $CF_3^+$ in the EBFlow, a small amount of $CH_3CH{=}CHF$ is recovered from the metathesis in equation 20 (followed by proton transfer to neutral propionaldehyde).[69] The principal $C_3H_5F$ isomer, though, is $CH_3CF{=}CH_2$, signalling that $(CH_3)_2CF^+$ has been formed. It is not altogether clear if all of that ion comes from isomerization of initially formed $CH_3CH_2CHF^+$, but the results outlined below show that at least some of it does. An EBFlow experiment with $^{13}C$-labeled propionaldehyde, summarized in equation 21, yields $CH_3CF{=}CH_2$ with $^{13}C$ in all positions (but not a random distribution). About one-fifth of the product has the label in the center carbon position, which must have arisen via unimolecular methyl shift within $CH_3CH_2CHF^+$.[88] The majority of ions, however, have come from a process that transposes fluorine.

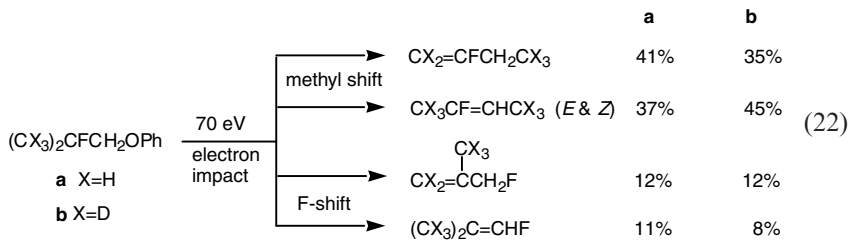


(22)

The first question posed at the beginning of this section inquires whether it is possible to distinguish atom transfer via a cyclic transition state from dissociation–recombination. An EBFlow study of unimolecular competition between methyl and fluorine shift, shown in equation 22, has addressed this issue.[73] The rearrangements occur in the course of forming ion–neutral complexes, and the product distributions change in going from unlabeled (**a**) to deuterated (**b**) starting material. A $^{19}F$ NMR measurement of the fluoroalkene distribution exhibits a degree of experimental error such that the ratio of F-shift products to methyl shift products cannot be said to change significantly with deuteration of the methyls, but statistically significant normal kinetic isotope effects are exerted on the distribution of positional isomers. The kinetic isotope effect on the ratios of the methyl shift products corresponds to $k_H/k_D = 1.4$ (with $k_H/k_D = 0.9$ on the $E/Z$ 2-fluorobutene product ratio), and for the F-shift products $k_H/k_D = 1.6$. These are consistent with the $PhOH^{\bullet+}$ : $PhOD^{\bullet+}$ ion intensity ratio observed

in the 70 eV mass spectrum of the deuterated ether. They represent the combined primary and $\alpha$-secondary isotope effects on the Brønsted acid–base reaction between the cation and the phenoxy radical in the complexes and are of the same magnitude as the isotope effects within the complexes shown in Scheme 15[69] as well as for deprotonation of cations within [*tert*-amyl cation PhO$^{\bullet}$] complexes from neopentyl phenyl ether.[34] They are smaller than the primary kinetic isotope effects reported for bimolecular hydride transfer.[80]

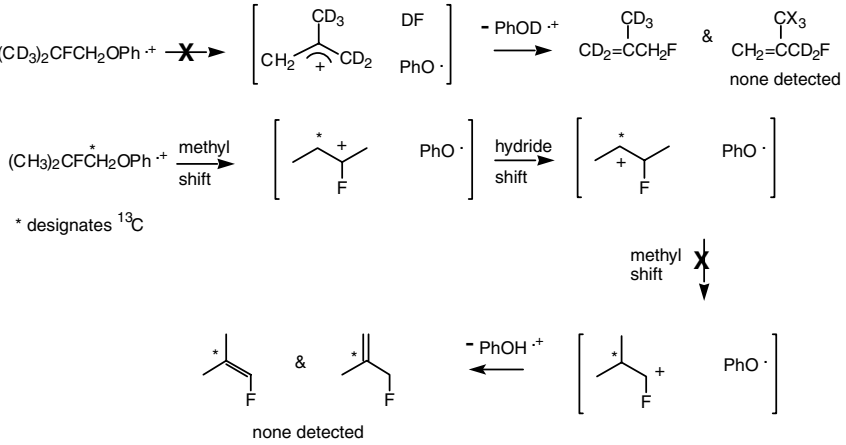


***Scheme 16.***

After correcting for reaction path degeneracies, methyl shift in equation 22 is approximately twice as likely as F-shift, compared with being three times as likely in the reaction summarized in Scheme 15. The absence of a significant isotope effect on methyl versus F-shift argues against a dissociation–recombination mechanism for F-shift. The deuterium labeling pattern in the neutral products rules out elimination–readdition rigorously. Had the transposition of fluorine occurred via the terbody complex drawn at the top of Scheme 16, neutral methallyl fluoride would have been recovered in which deuterium is attached to the same carbon as fluorine, but that product is not seen. The $^{13}$C-labeling experiment summarized at the bottom of Scheme 16 confirms this and also demonstrates that a genuine fluorine shift has taken place, instead of the carbon skeleton rearrangement shown, which would not have attached fluorine to the tagged carbon. Both of the branched products from the $^{13}$C-labeled precursor display NMR spin–spin couplings proving that fluorine is directly connected to the tagged carbon, while the linear fluorobutenes show only two-bond couplings between $^{19}$F and $^{13}$C.[72]

The second question raised at the beginning of this section asks which atom/group transfers proceed via reversible ring closure to a stable intermediate. Some cationic ring closures are irreversible (at least, on the timescale of the reactions that produce the recovered neutral products); for instance, equations 16 and 19. While SCF calculations predict that the epifluoronium ion in equation 19 lies in a potential energy well, they indicate that unsymmetrical alkyl substitution of the 3-membered ring destabilizes the cyclic structure so that it becomes a transition state.[72] If that is correct, the F-shifts in Scheme 15 and equation 22 pass through cyclic transition states and do not operate by reversible ring closure-ring opening.

F-shift exhibits two limiting cases: in one instance a ring closes, but does not open again until a base pulls a proton off from the epifluoronium ion; in other instances, the ring does not correspond to a minimum on the potential energy surface. In a number of different systems a variety of options are equally plausible, and experiment draws a distinction that theory cannot. For example, the results summarized in Scheme 9 argue that hydride shift from one carbon to the other in equation 15 does not proceed via ring closure to protonated ethylene oxide followed by ring opening concomitant with a hydrogen transposition.

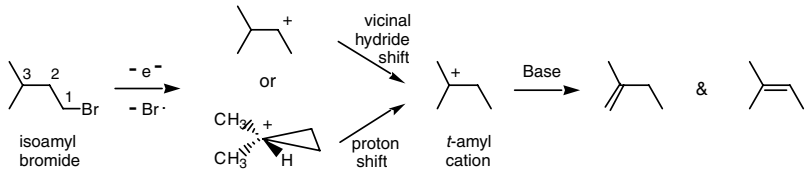


***Scheme 17.***

A number of cases remain to be resolved where theory gives an equivocal answer, such as in the formation of *t*-amyl cation from ionization of isoamyl bromide. An EBFlow experiment provides evidence for the net reaction illustrated in Scheme 17: 70 eV radiolysis of 0.0005 mbar isoamyl bromide plus 0.0003 mbar triethylamine yields 2-methyl-1-butene as the principal $C_5H_{10}$ product (2.3 μmol/A-s) with a slightly lower yield of 2-methyl-2-butene.[15] Rearrangement takes place in the course of loss of a bromine atom from the molecular ion. At least two different mechanisms can describe what takes place. Vicinal hydride shift could occur to make a secondary isoamyl cation, $(CH_3)_2CHCHCH_3^+$, which might undergo another vicinal hydride shift to give *t*-amyl cation. Alternatively, a corner-protonated cyclopropane might form, which could undergo a corner-to-corner proton shift and open up to make the *t*-amyl cation. DFT calculations predict both intermediates

to be stable, with the secondary cation 30 kJ/mol more stable than the corner-protonated cyclopropane. Successive vicinal hydride shifts predict a different isotopic substitution pattern on the *t*-amyl than does the net 1,3-transfer implied by the protonated cyclopropane intermediate, but the barrier for unimolecular randomization of all the hydrogens within *t*-amyl cation is so low as to render an isotopic labeling experiment problematic.[68] In any event, specific deuteration of isoamyl bromide at carbon 3 did not succeed in distinguishing the two pathways, since label scrambling within the $C_5H_9D^{\bullet+}$ parent ions foiled any attempt to use GC-MS to determine the position of the isotope in recovered 2-methyl-1-butene.

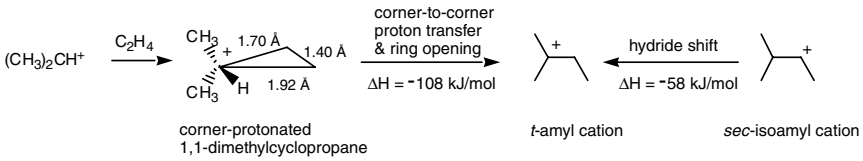


***Scheme 18.***

A different type of experiment demonstrates the viability of an intermediate protonated cyclopropane. Isopropyl cation ($i\mathrm{Pr}^+$) was generated in the EBFlow by 70 eV electron bombardment of di-*n*-propyl ether (0.0004 mbar) in the presence of ethylene (0.0013 mbar). This reaction yields 0.09 μmol/A-s of 2-methyl-1-butene and 0.08 μmol/A-s of 2-methyl-2-butene.[15] Ion–molecule association reactions are ordinarily extremely inefficient at these low pressures because, in the absence of a third body collision, the cluster ion has enough internal energy to dissociate back to the reactants. But, as Scheme 18 depicts, $i\mathrm{Pr}^+$ associates with ethylene to make *t*-amyl cation. It seems unlikely that this reaction passes through the *sec*-isoamyl cation, even though DFT calculations (summarized in Scheme 18) predict it to be 50 kJ/mol more stable than the corner-protonated cyclopropane. Formation of an intermediate *sec*-isoamyl cation would require migration of one of the hydrogens originally attached to ethylene.

DFT calculations show that the corner-protonated cyclopropane has the structure shown in Scheme 18. Its geometry that resembles an $i\mathrm{Pr}^+$ sitting on top of an ethylene, but with the charge-bearing carbon pyramidalized. Rearrangement to *t*-amyl cation is highly exothermic. RRKM estimates of the rate of corner-to-corner proton transfer suggest that isomerization occurs rapidly enough to compete with dissociation.[68] Given that the experimental value for the net exothermicity of $i\mathrm{Pr}^+ + C_2H_4 \rightarrow$ *t*-amyl cation has a value of $\Delta H = -140$ kJ/mol, rearrangement puts $C_5H_{11}^+$ into such a deep well that it can last for milliseconds without dissociating. But, in the absence of rearrangement, RRKM calculations predict a lifetime

for the corner-protonated cyclopropane $<10^{-8}$ s (to be compared with experimental estimates on the order of a fraction of a nanosecond for the lifetimes of ion–neutral complexes[36,78]). If these estimates are correct, corner-to-corner proton transfer concomitant with ring opening must be at least as fast as RRKM calculations predict.

According to the rules of orbital symmetry, vicinal hydride shift in cations is a thermally allowed suprafacial 1,2-sigmatropic shift. Migration of a more distant hydrogen can occur by successive 1,2-shifts,[89] via a bridged structure (such as the cyclooctyl cation in Scheme 7[35]), or by corner-to-corner transfer in a protonated cyclopropane (which give net 1,3-shifts). An EBFlow experiment has been able to measure the competition between 1,2- and 1,3-shift in the 1-fluoropropyl system.

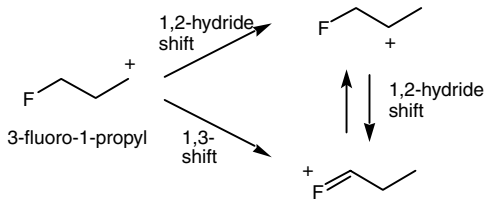


***Scheme 19.***

The 3-fluoro-1-propyl cation is not a stable species. It rearranges, as Scheme 19 portrays, to a mixture of two cations that have nearly the same stability (cf. Scheme 15 above). This isomerization can occur via two pathways—a 1,3-shift or successive 1,2-shifts. Experimentally, these pathways have been distinguished by looking at the EBFlow of $PhOCH_2CH_2CD_2F$, which forms ion–neutral complexes by C–O bond heterolysis (cf. equation 18). A 1,2-shift transfers hydrogen to form a methyl group. A 1,3-shift transfers deuterium directly to form a $CH_2D$ group. Subsequent 1,2-shifts (which interconvert the two stable isomers drawn to the right in Scheme 19) do not affect the labeling pattern of the methyl. The $^{19}F$ NMR of the recovered neutral 1-fluoropropenes in Figure 4 shows that products with undeuterated methyl groups are 15 times more abundant than products with $CH_2D$-groups, which is taken to represent the relative rates of 1,2- versus 1,3-shift.[71]

A striking feature of this EBFlow radiolysis experiment is the low yield of 2-fluoropropene, all of which can be accounted for by the small amount of free fluoropropyl ions generated by 70 eV electron impact. This result implies that the skeletal rearrangement of linear to branched fluoropropyl cations (which gives rise to the neutral products in equation 21, for example) occurs too slowly to take place in the brief lifetime of ion–neutral complexes. In this regard the ion–neutral complexes formed by ionizing

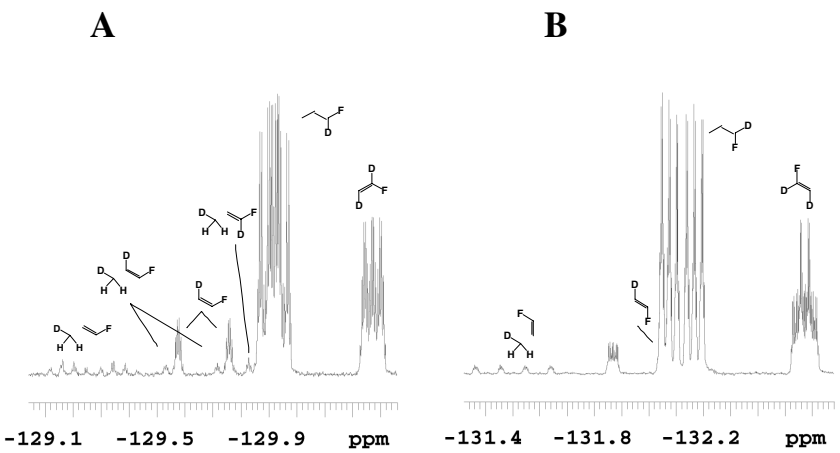


***Figure 4.*** $^{19}$F NMR spectrum of 1-fluoropropenes (**A** *trans*; **B** *cis*) from 70 eV EBFlow radiolysis of $PhOCH_2CH_2CD_2F$.

3-fluoropropyl phenyl ether closely parallel the behavior of complexes from *n*-butyl phenyl ether,[61] just as equation 22 parallels ionized neopentyl phenyl ether.[34] These outcomes support the view that, in a carbocation, a single fluorine substituent has many of the same properties as a methyl group.

## V. CONCLUSION

Cationic rearrangements display considerable variety. Investigations of the simplest molecular systems have proven difficult in condensed phases but have been amenable to systematic study in the gas phase. Neutral product studies exhibit the scope and limitations of two general categories of isomerization—ring closure/ring opening and atom/group transfer—and do not suggest that any additional categories need be added to the repertoire. In terms of unimolecular reaction rates, three general classes of reactions operate: rearrangements that take place concomitantly with bond heterolyses, those that occur rapidly after heterolysis and whose neutral products can be detected from ion–neutral complexes, and those that happen in free cations but which are too slow to be observed to any great extent within complexes. Radiolytic and mass spectrometric studies (in which bonds heterolyze following ionization) find their complement in tritium decay studies (in which helium departs as a leaving group so rapidly that

heterolysis is virtually simultaneous with ionization, and rearrangement occurs later).

At present, theory has developed a persuasive ability to predict cation stabilities. Current understanding of relative reaction rates, however, has not advanced as far. A number of processes for which computation predicts no energy barrier (such as the ring closure in equation 19 or the collapse of ion–neutral complexes to give rearranged, covalently bound ions[28]) occur slowly relative to reactions (such as hydride shift or proton transfer) that would appear to have low (but nonzero) potential energy barriers. Neutral product distributions give a view of the dynamics of competing reactions that is difficult to acquire by any other means. The long-term objectives of such experiments include an understanding of competing pathways that would permit an organization of reactions within enzyme active sites along the lines of the three classes listed above.

## ACKNOWLEDGMENT

This work was supported by NSF grant CHE 9983610.

## REFERENCES

[1] Coates, R.M. *Prog. Chem. Org. Nat. Prod.* **1976**, *33*, 74–230.
[2] Gibbs, R.A. In *Comprehensive Biological Catalysis: a Mechanistic Reference*; Vol 1 Sinnott, M., Ed.), Academic Press., 1998, p 31–118.
[3] Bohlmann, J.; Meyer-Gauen, G.; Croteau, R. *Proc. Nat. Acad. USA* **1998**, *95*, 4126–4133.
[4] Hoshino, T.; Abe, T.; Kouda, M. *JCS Chem. Commun.* **2000**, 441–442; Dang, T.; Prestwich, G.D. *Chemistry& Biology* **2000**, *7*, 643–649; Fernandez, S.M.S.; Kellogg, B.A.; Poulter, C.D. *Biochemistry* **2000**, *39*, 15316–15321; Wendt. K.U.; Schulz, G.E.; Corey, E.J.; Liu, D.R. *Angew. Chem. Int. Ed.* **2000**, *39*, 2812–2833.
[5] Kohn, W.; Becke, A.D.; Parr, R.G. *J. Phys. Chem.* **1996**, *100*, 12974–12980.
[6] Morton,T.H.; Beauchamp, J.L. *J. Am. Chem. Soc.* **1975**, *97*, 2355–2362; **1977**, *99*, 1288.
[7] Maslak, P.; McGuinn, J.M. *JCS Chem. Commun.* **1999**, 2467–2468.
[8] Baciocchi, E; Bietti, M.; Lanzalunga, O. *Acc. Chem. Res.* **2000**, *33*, 243–251.
[9] Stevenson, D.P. *Disc. Faraday Soc.* **1951**, *10*, 35–45.
[10] Audier, H.E. *Org. Mass Spectrom.* **1969**, *2*, 283–298.
[11] Coulson, D.R. *J. Am. Chem. Soc.* **1978**, *100*, 2992–2996.
[12] Pollak, E.; Pechoukas, P. *J. Am. Chem. Soc.* **1978**, *100*, 2984–2991.
[13] Weddle, G.H.; Dunbar, R.C.; Song, K.; Morton, T.H. *J. Am. Chem. Soc.* **1995**, *117*, 2573–2580.
[14] Traeger, J.C.; Luna, A.; Tortajada, J.C.; Morton, T.H. *J. Phys. Chem. A* **1999**, *103*, 2348–2358.
[15] Marinelli, W.J.; Morton, T.H. *J. Am. Chem. Soc.* **1978**, *100*, 3536–3539; **1979**, *101*, 1908.
[16] Attiná, M.; Cacace, F.; Cipollini, R.; Speranza, M. *J. Am. Chem. Soc.* **1985**, *107*, 4824–4828.
[17] Attiná, M.; Cacace, F.; DiMarzio, A. *J. Am. Chem. Soc.* **1989**, *111*, 6004–6008.

[18] Morton, T.H. In *Techniques for the Study of Ion-Molecule Reactions*; Farrar, J.M.; Saunders, W.H. Jr., Ed., *Techniques of Chemistry XX*, Wiley-Interscience, New York, 1988, p 119–164.
[19] Redman, E.W.; Morton, T.H. *J. Am. Chem. Soc.* **1986**, *108*, 5701–5708.
[20] Taphanel, M.H.; Morizur, J.P.; Leblanc, D.; Borchardt, D.; Morton, T.H. *Anal. Chem.* **1997**, *69*, 4191–4196.
[21] Morizur, J.P.; Taphanel, M.H.; Mayer, P. S.; Morton, T. H. *J. Org. Chem.* **2000**, *65*, 381–387.
[22] Biermann, H.W.; Freeman, W.P.; Morton, T.H. *J. Am. Chem. Soc.* **1982**, *104*, 2307–2308.
[23] Andlauer, B.; Ottinger, Ch. *J. Chem. Phys.* **1971**, *55*, 1471–1472.
[24] Fairweather, R.B.; McLafferty, F.W. *Org. Mass Spectrom.* **1970**, *4*, 221–224.
[25] Kondrat , R.W.; Morton, T.H. *Org. Mass Spectrom.* **1991**, *26*, 410–415.
[26] Chronister, E.L.; Morton, T.H. *J. Am. Chem. Soc.* **1990**, *112*, 133–139.
[27] Song, K.; van Eijk, A.; Shaler, T.A.; Morton, T.H. *J. Am. Chem. Soc.* **1994**, *116*, 4455–4460.
[28] Traeger, J.C.; Morton, T.H. *J. Am. Chem. Soc.* **1996**, *118*, 9661–9668.
[29] Kohler, B.E.; Morton, T.H.; Nguyen, V.; Shaler, T.A. *J. Phys. Chem. A* **1999**, *103*, 2302–2309
[30] Morton, T.H. *Org. Mass Spectrom.* **1992**, *27*, 353–368.
[31] Abboud, J.M.; Alkorta, I.; Dávalos, J.Z.; Gal, J.-F.; Herreros, M.; Maria, P.-C.; Mó, O.; Molina, M.T.; Notario, R.; Yañez, M. *J. Am. Chem. Soc.* **2000**, *122*, 4451–4454.
[32] Illies, A.J.; Morton, T.H. *Int. J. Mass Spectrom. Ion Processes* **1997**, *167/168*, 431–445.
[33] Midland, M.M.; Morton, T.H. *J. Am. Chem. Soc.* **1993**, *115*, 9596–9601.
[34] Morton, T.H. *J. Am. Chem. Soc.* **1980**, *102*, 1596–1602.
[35] Kirchen, R.P.; Sorenson, T.S. *J. Am. Chem. Soc.* **1979**, *101*, 3240–3243.
[36] Aschi, M.; Attiná, M.; Cacace, F.; D'Archangelo, G. *J. Am. Chem. Soc.* **1998**, *120*, 3982–3987.
[37] Audier, H.E.; Morton, T.H. *J. Am. Chem. Soc.* **1991**, *113*, 9001–9003.
[38] Morton, T.H. *Tetrahedron* **1982**, *38*, 3195–3243.
[39] McAdoo, D.J.; Morton, T.H. **1993**, *26*, 295–302.
[40] Cacace, F.; Speranza, M. In *Techniques for the Study of Ion–Molecule Reactions*; Farrar, J.M., Saunders, W.H., Jr., Eds.; *Techniques of Chemistry XX*; Wiley-Interscience, New York, 1988, p. 287–323.
[41] Cacace, F. *Science* **1990**, *250*, 392–399.
[42] Speranza, M. *Chem. Rev.* **1993**, 2833–2986.
[43] Nefedov, V.D.; Sinotova, E.N.; Akulov, G.P.; Korsakov, M.V. *J. Org. Chem. USSR* **1970**, *6*, 1220–1224.
[44] Smith, R.D.; Herold, D.A.; Elwood, T.A.; Futrell, J.H. *J. Am. Chem. Soc.* **1977**, *99*, 6042–6045.
[45] Nefedov, V.D.; Sinotova, E.N.; Bermudez, R.K. *J. Org. Chem. USSR* **1982**, *18*, 1642–1646.
[46] Hudson, C.E.; McAdoo, D.J. *J. Am. Soc. Mass Spectrom.* **1998**, *9*, 130–137.
[47] Cacace, F.; Ciranni, G.; Sparapani, C.; Speranza, M. *J. Am. Chem. Soc.* **1984**, *106*, 8046–8050.
[48] Filippi, A.; Lilla, G.; Occhiucci, G.; Sparapani, C.; Ursini, O.; Speranza, M. *J. Org. Chem.* **1995**, *60*, 1250–1264.
[49] Fornarini, S.; Speranza, M. *J. Chem. Soc. Perkin 2* **1984**, 171–177.
[50] Benoit, F.M.; Harrison, A.G. *Org. Mass Spectrom.* **1976**, *11*, 599–608.
[51] Bogdanov, B.; Matimba, H.E.K.; Ingemann, S.; Nibbering, N.M.M. *J. Am. Soc. Mass Spectrom.* **1996**, *7*, 639–652.
[52] Kondrat, R.W.; Morton, T.H. *J. Org. Chem.* **1991**, *56*, 952–957.

[53] Jacquet, J.-P.; Morton, T.H. *J. Mass Spectrom.* **1997**, *32*, 251–252.
[54] Nguyen, V.; Bennett, J.S.; Morton, T.H. *J. Am. Chem. Soc.* **1997**, *119*, 8342–8349; **1997**, *119*, 12026.
[55] Mayer, P.; Morton, T.H. Paper presented at the 46th ASMS Conference on Mass Spectrometry and Allied Topics, Dallas, TX, June, 1999; manuscript in preparation.
[56] Zhao, L.; Chronister, E.L.; Morton, T.H. Unpublished results.
[57] Ausloos, P.; Lias, S.G. *J. Am. Chem. Soc.* **1970**, *92*, 5037–5045.
[58] Cacace, F. *Acc. Chem. Res.* **1988**, *21*, 215–222.
[59] Speranza, M. *Mass Spectrom. Rev.* **1992**, *11*, 73–117.
[60] Doepker, R.D.; Ausloos, P. *J. Chem. Phys.* **1965**, *43*, 3814–3819.
[61] Burns, F.B.; Morton, T.H. *J. Am. Chem. Soc.* **1976**, *98*, 7308–7313.
[62] Fornarini, S.; Muraglia, V. *J. Am. Chem. Soc.* **1989**, *111*, 873–877.
[63] Laguzzi, G.; Angelini, G.; Bucci, R.; Segre, A.L. *J. Phys. Chem.* **1994**, *98*, 6719–6724.
[64] Cacace, F.; Speranza, M. *J. Am. Chem. Soc.* **1979**, *101*, 1587–1589.
[65] Cacace, F.; Chiavarino, F.B.; Crestoni, M.E. *Chem. Eur. J.* **2000**, *6*, 2024–2031.
[66] Babérnics, L.; Cacace, F. *J. Chem. Soc. B* **1971**, 2312–2316.
[67] Audier, H.E.; Leblanc, D.; Mayer, P.S.; Morton, T.H. *European Mass Spectrom.* **2000**, *5*, 419–429.
[68] Morton, T.H. *Radiat. Phys. Chem.* **1982**, *20*, 29–40.
[69] Shaler, T.A.; Morton, T.H. *J. Am. Chem. Soc.* **1991**, *113*, 6771–6779.
[70] Nguyen, V.; Cheng, X.; Morton, T.H. *J. Am. Chem. Soc.* **1992**, *114*, 7127–7132.
[71] Shaler, T.A.; Borchardt, D.; Morton, T.H. *J. Am. Chem. Soc.* **1999**, *121*, 7907–7913.
[72] Shaler, T.A.; Morton, T.H. *J. Am. Chem. Soc.* **1994**, *116*, 9222–9226.
[73] Shaler; T.A.; Morton, T.H. *J. Am. Chem. Soc.* **1989**, *111*, 6868–6870; **1990**, *112*, 4090.
[74] Beckwith, A.L.J.; Eaton, C.J.; Lawrence, T.; Serelis, A.K. *Aust. J. Chem.* **1983**, *36*, 545–556.
[75] Grandinetti, F.; Occhiucci, G.; Crestoni, M.E.; Fornarini, S.; Speranza, M. *Int. J. Mass Spectrom. Ion Processes* **1993**, *127*, 123–135.
[76] Grandinetti, F.; Occhiucci, G.; Crestoni, M.E.; Fornarini, S.; Speranza, M. *Int. J. Mass Spectrom. Ion Processes* **1993**, *127*, 137–146.
[77] Grandinetti, F.; Crestoni, M.E.; Fornarini, S. and Speranza, M. *Int. J. Mass Spectrom. Ion Processes* **1994**, *130*, 207–222.
[78] Aschi, M.; Attiná, M.; Cacace, F. *Chem. Eur. J.* **1998**, *4*, 1535–1541.
[79] Crestoni, M.E.; Fornarini, S.; Lentini, M.; Speranza, M. *Chem. Commun.* **1995**, 121–122.
[80] Crestoni, M.E.; Fornarini, S.; Lentini, M.; Speranza, M. *J. Phys. Chem.* **1996**, *100*, 8285–8294.
[81] Johnson, W.S.; Chenera, B.; Tham, F.S.;. Kullnig, R.K. *J. Am. Chem. Soc.* **1993**, *115*, 493–497.
[82] Johnson, W.S.; Buchanan, R.A.; Bartlett, W.R.; Tham, F.S.; Kullnig, R.K. *J. Am. Chem. Soc.* **1993**, *115*, 504–515.
[83] Eyler, J.R.; Ausloos, P.; Lias, S.G. *J. Am. Chem. Soc.* **1974**, *96*, 3673–3675.
[84] Ausloos, P.; Lias, S.G.; Eyler, J.R. *Int. J. Mass Spectrom. Ion Processes* **1975**, *18*, 261–271.
[85] Redman, E.W.; Johri, K.K.; Lee, R.W.K.; Morton, T.H. *J. Am. Chem. Soc.* **1984**, *106*, 4639–4640.
[86] Redman, E.W.; Johri, K.K.; Morton, T.H. *J. Am. Chem. Soc.* **1985**, *107*, 780–784.
[87] Stams, D.A.; Johri, K.K.; Morton, T.H. *J. Am. Chem. Soc.* **1988**, *110*, 699–706.
[88] Nguyen, V.; Mayer, P.S.; Morton, T.H. *J. Org. Chem.* **2000**, *65*, 8032–8040.
[89] Sorensen, T.S.; Whitworth, S.M. *J. Am. Chem. Soc.* **1990**, *112*, 6647–6651.